UNIVERSITÀ POLITECNICA DELLE MARCHE
Repository ISTITUZIONALE

Expeditious methodology for the estimation of infill masonry wall stiffness through in-situ dynamic tests

This is the peer reviewd version of the followng article:

Original
Expeditious methodology for the estimation of infill masonry wall stiffness through in-situ dynamic tests / Nicoletti, V.; Arezzo, D.; Carbonari, S.; Gara, F.. - In: CONSTRUCTION AND BUILDING MATERIALS. - ISSN 0950-0618. - 262:(2020). [10.1016/j.conbuildmat.2020.120807]

Availability:
This version is available at: 11566/283984 since: 2024-04-28T09:35:55Z

Publisher:

Published
DOI:10.1016/j.conbuildmat.2020.120807

Terms of use:

The terms and conditions for the reuse of this version of the manuscript are specified in the publishing policy. The use of copyrighted works requires the consent of the rights' holder (author or publisher). Works made available under a Creative Commons license or a Publisher's custom-made license can be used according to the terms and conditions contained therein. See editor's website for further information and terms and conditions.
This item was downloaded from IRIS Università Politecnica delle Marche (https://iris.univpm.it). When citing, please refer to the published version.

note finali coverpage

(Article begins on next page)

26 May 2024

Expeditious Methodology for the Estimation of Infill Masonry Wall Stiffness Through in-situ Dynamic Tests

Vanni Nicoletti[a], Davide Arezzo[a], Sandro Carbonari[a][1], Fabrizio Gara[a]

[a] Dept. ICEA, Università Politecnica delle Marche, Via Brecce Bianche, 60131 Ancona, Italy.
E-mail: v.nicoletti@pm.univpm.it, d.arezzo@pm.univpm.it, s.carbonari@univpm.it, f.gara@univpm.it

Abstract

In this paper a procedure to experimentally estimate the stiffness of masonry internal partitions and infill walls is proposed with the aim of providing a practical tool to reduce uncertainties in the finite element modelling of frame buildings when partitions and infills must be included. The proposed methodology, based on in-situ impact load tests and numerical modelling, is presented. The methodology is validated through an experimental campaign on a laboratory mock-up and applied to a real reinforced concrete frame building. The proposed methodology revealed capable to provide a very accurate estimate of the infill stiffness to be adopted in the building modelling.

Keywords: Infill masonry wall stiffness, impact load test, experimental modal analysis, operational modal analysis, building f.e. modelling, experimental methodology.

1. Introduction

Infill walls have been considered for a long time non-structural elements whose influence in the structural response may be neglected, both in terms of stiffness and strength. This practice was supported by the hypothesis that at Ultimate Limit States (ULSs) infill walls are usually assumed to be completely damaged, so that their contribution is negligible in terms of stiffness and strength, while at Damage Limit States (DLSs), a conservative evaluation of the interstorey drifts, on which verifications are based, is achieved if infill walls are neglected. Nowadays, it is accepted by the overall scientific and technical communities that the stiffness and strength provided by these non-structural elements must be considered in the numerical models for the assessment of reinforced concrete (r.c.) structures because they may significantly affect the global behaviour of buildings, especially in earthquake-prone areas [1-5]. Indeed, detrimental dynamic interactions between structural and non-structural components may be responsible of premature structural failures and may prevent the correct evolution of dissipative mechanisms [6-8].

[1] Corresponding author, Department of Civil and Building Engineering, and Architecture, DICEA, Università Politecnica delle Marche, Via Brecce Bianche, 60131 Ancona, Italy - E-mail address: s.carbonari@univpm.it

Furthermore, for strategic buildings (e.g. schools, hospitals, police and fire stations, government buildings) it may be crucial to limit the infill walls damage even for severe earthquake, in order to guarantee the building occupancy during the emergency management [9]. For this reason, strategic buildings are often seismically protected with isolation and dissipative systems which must be designed taking into account the real dynamic behaviour of the structure [10] that is strongly affected by the stiffening contribution of infills. For existing structures, which must be seismically upgraded, dynamic identification tests are generally performed to achieve the required level of knowledge and to calibrate the finite element (f.e.) model developed for the design of the seismic protection system; this implies that the contribution of non-structural elements is included in the numerical model.

Finally, the Structural Health Monitoring (SHM) of buildings requires the setup of a numerical model representative of the building operational condition through which any measured change of the structural behaviour is interpreted [11-13]. Obviously, the contribution of non-structural components must be considered, also considering that the identification of their damage may be of interest.

Taking into account above needs, many numerical models have been developed for the modelling of the infills, ranging from the simple replacement of the wall by one or more equivalent diagonal struts [14-19], to detailed linear and nonlinear f.e. models [20-22]. However, parameter and modelling uncertainties exist and affect the accuracy of such models because the infill behaviour depends on several aspects, such as the mechanical properties of materials and the geometric dimensions, the presence of openings, and the construction techniques [23-26].

Most of researchers investigated the in-plane behaviour of infill masonry walls subjected to static and cyclic loads with the aim of providing empirical drift capacity models to characterize the elastic and post-elastic performance of infills [27-32]. However, these tests led to a large variety of results because of the large variety of construction materials (types and quality) and techniques. Indeed, dimensions and material composition of bricks, mortar characteristics, as well as construction practices may differ sensibly from one region to another, so that a standardization is almost impossible [33-35]. Dynamic tests have been also used in the literature to characterise infill panels [36]. However, only few works deal with the investigation of the infills dynamic properties, mainly focusing on the influence of damage and openings in the out-of-plane response [37].

The aim of this paper is to propose a practical procedure to reduce uncertainties in the f.e. modelling of buildings including infill masonry walls. While the mass of masonry panels can be reasonably estimated, great uncertainties are generally related to their stiffening contribution that can vary in a large range. The proposed methodology foresees dynamic Impact Load Tests (ILTs) from which the modal parameters of the out-of-plane response of the masonry panel are identified. The latter are used to estimate an infill equivalent elastic modulus that can be adopted in a conventional 3-D f.e.

modelling of these non-structural elements in the linear range. Tests are fast and non-invasive so that they can be easily and widely executed on existing structures. At first, the proposed combined experimental and numerical methodology is presented and then validated through experimental and numerical studies performed on a laboratory mock-up. The latter consists in a simple one floor steel frame structure with a steel-concrete composite slab, which is investigated without and with the presence of infill masonry walls. The reliability of the proposed methodology for the estimation of the infill stiffness is assessed through comparisons between numerical and experimental modal parameters of the whole structure, the latter derived from Ambient Vibration Tests (AVTs). Finally, the proposed methodology is applied to a real infilled r.c. frame building investigated during its construction, taking advantage of results of AVTs performed on both the bare and infilled frame.

2 The proposed simplified methodology

The proposed methodology, based on a combined experimental and numerical procedure, has the goal to estimate an equivalent elastic modulus for the infill masonry panels which are modelled on 3-D f.e. models of buildings through shell elements. Despite masonry infills are generally characterised by an orthotropic behaviour, the method stems from the idea that the dynamic behaviour of infills subjected to low input excitations can be well captured through homogenous isotropic elastic thin plates, so that the in-plane and out-of-plane response is governed by the same mechanical parameters. The term equivalent incorporates the aforementioned simplified assumptions, as well as a geometric issue relevant to modelling practices, which usually foresee the use of 2-node beam elements for the r.c. members (beams and columns). In this sense, the modulus defines the material of the elements that are used to fill-in the bare structure, neglecting thicknesses of structural elements. Thus, the methodology does not allow for a rigorous estimation of the mechanical properties of the orthotropic panel but rather those of an equivalent material that can be employed to capture the overall dynamic contribution of the infills in a 3-D f.e. structural model. The methodology, schematically depicted in Figure 1, is based on a two-step procedure, involving both an experimental and a numerical step: the former requires the execution of ILTs on the wall without openings that has to be identified, and the latter foresees the wall modelling for the elastic modulus calibration.

2.1 Experimental Step

As concerns the experimental step (Figure 1), ILTs are performed on the infill masonry wall to identify its out-of-plane dynamic behaviour. Test consists in exciting the panel with a hammer blow applied in the direction orthogonal to the wall plane, and in recording the time history of the impulse and that of the produced acceleration in the same direction. Tests should be performed with the aim of

identifying accurately modal parameters of the out-of-plane response (resonance frequencies and mode shapes) extending the identification also to superior modes. To this purpose, impulses can be provided in one or more panel positions, as well as the accelerations can be measured in one or more points, depending on the adopted test and post-processing procedures. Herein, the following procedure, used in the sequel for the validation and application of the proposed method, is suggested to get a detailed modal identification for the tested infills, identifying several resonant frequencies and mode shapes that characterize the out-of-plane dynamic behaviour of the walls. The masonry panel is divided with a regular grid of twenty-five points (Figure 2) and two accelerometers (ACC1 and ACC2) are placed in different grid points (C3 and B2, respectively). Two sensors in different positions are employed instead of one in order to identify with redundancy a significant number of modes, and, moreover, to allow the identification of also those modes that have null value of the modal displacement in proximity of one of the two sensors. In this sense, the sensor placement is not univocal and preliminary tests can be performed to evaluate the best positions to capture the first modes of the infills. During the tests, the impulsive forces are applied at each grid point while accelerometers are left in the same positions. Finally, for each of the twenty-five grid points, a set of three or more hammer blows is applied in order to get a reliable data set. The data collected from these tests can be used to perform Single-Input Single-Output (SISO) or Single-Input Multi-Output modal analysis since the accelerations are simultaneously recorded at two points by exciting the element in only one point at a time. Hence, as a result, the modal parameters that characterize the out-of-plane dynamic behaviour of the panel are obtained. In this work, the modal identification technique adopted to perform the modal analysis is the "Line-Fit" algorithm [38-39], which is a SDOF methodology working in the frequency domain. The modal analysis developed is a SISO analysis, namely the records of only one accelerometer are considered in the algorithm for each of the twenty-five set of impulses. Consequently, initially two different modal identifications are performed for each tested wall, then the wall modal parameters are obtained by comparing and merging the results of the two modal analyses.

2.2 Numerical Step

As for the numerical step of the proposed procedure (Figure 1), it starts from the conventional f.e. model of the bare structure that is usually available and needs to be refined with the contribution of non-structural components for the problem at hand. The investigated infills are included as bidimensional thin shell elements in the bare frame model, including adjacent ones, which may contribute to a correct modelling of the boundary conditions (i.e. restraint conditions) for the investigated walls. The material is assumed to be homogeneous and isotropic whereas the mass per unit area ρ of the plate is evaluated with a reasonable accuracy by considering the wall layout and thicknesses. By assuming a conventional

nominal value for the Poisson's ratio ν (e.g. 0.25 as suggested in [40]), the resonance frequencies and mode shapes of the plate are only governed by the elastic modulus E of the shell material. Whereupon, a tentative elastic modulus E_0 for the masonry panel is estimated; closed-form expressions available in the literature for clamped rectangular plates can be profitably used to evaluate a tentative value starting from the fundamental frequency of the wall evaluated from experimental tests. As an example, according to [41], the following simple frequency formula holds for clamped rectangular homogeneous isotropic thin plates

$$f^2 = \frac{\pi^2 E_0 t^2}{48\rho(1-\nu^2)}\left[\left(\frac{m+\Delta_m}{a}\right)^2 + \left(\frac{n+\Delta_n}{b}\right)^2\right]^2 \quad (1)$$

where ρ is the plate mass per unit area, t is the plate thickness, ν is the Poisson's ratio, a and b are the plate geometric dimensions, and f is the vibration frequency. In Equation (1), m and n are the numbers of ½ waves in the mode shapes in the two principal directions while Δm and Δn are the so-called "edge effect factors" that can be expressed as a function of the mode number and the plate dimensions according to

$$\Delta_m = \left[\left(\frac{n\cdot a}{m\cdot b}\right)^2 + 2\right]^{-1} + \left(\frac{0.017}{m}\right) \quad (2a)$$

$$\Delta_n = \left[\left(\frac{m\cdot b}{n\cdot a}\right)^2 + 2\right]^{-1} + \left(\frac{0.017}{n}\right) \quad (2b)$$

Thus, with reference to the fundamental vibration mode (i.e. m = 1 and n = 1), Equation (1) provides the tentative elastic modulus

$$E_0 = \frac{48\rho(1-\nu^2)}{\pi^2 t^2} f_{1,exp}^2 \left[\left(\frac{1+\Delta_{m=1}}{a}\right)^2 + \left(\frac{1+\Delta_{n=1}}{b}\right)^2\right]^{-2} \quad (3)$$

Usually, the tentative value E_0 is lower than the equivalent one E, since the real restraint conditions for the panel, which depend on the torsional and flexural stiffnesses of the frame as well as on the contribution of adjacent panels, do not assure absence of rotations and displacements of the infill contours, even for low energy excitations. According to the authors' experience, small variations of the boundary restraint conditions can largely affect the frequency values. Although a significant number of works are available in the literature addressing the problem of the frequency evaluation of plates with different boundary conditions [42-43], including elastic ones [44-45], the proposed methodology foresees a f.e. model based iterative approach due to the inherent difficulties in the definition of the real elastic boundary conditions for the infill when subjected to low energy impact forces. In fact, such boundary conditions depend not only on the geometry of the problem and the typology of infill walls, but also on the adopted construction procedures. Resonant frequencies and mode shapes that characterise the out-of-plane response of the investigated infills are determined numerically through eigenvalue analyses and the equivalent elastic modulus E of the infills is iteratively adjusted in order to minimize

differences between the experimental (exp) and numerical (num) modal parameters. Focusing on both frequency values and mode shapes, the following convergence criteria can be considered

$$\frac{\sum_{i=1}^{N}\frac{1}{i}\left|\frac{f_{i.exp}-f_{i.num}}{f_{i.exp}}\right|}{\sum_{i=1}^{N}1/i} \leq \delta_f \tag{4a}$$

$$1-\frac{\sum_{i=1}^{N}\frac{MAC_i}{i}}{\sum_{i=1}^{N}1/i} \leq \delta_s \tag{4b}$$

where $f_{i,exp}$ and $f_{i,num}$ are the experimental and numerical values of the *i*-th frequency and MAC_i (Modal Assurance Criterion index [46]) is a scalar indicator that expresses the similarity between the numerical and experimental mode shapes relevant to the *i*-th mode (0, no matching, 1 perfect match). In Equations (4), *N* is the number of vibration modes on which the calibration is based while δ_f and δ_s are the admissible percentage errors in the comparisons of frequencies (*f*) and mode shapes (*s*). It is worth noting that the comparison of experimental and numerical results is weighted, being the weight inversely proportional to the mode number. Herein, values around δ_f = 5% and δ_s = 25% are suggested and will be adopted in the method validation and applications of the following sections. The iterative procedure stops when both convergence criteria (Equation (4a) and (4b)) are matched.

As previously observed, when infills are included in the r.c. frame structures, usually the physical dimensions of the r.c. member cross sections are neglected so that the modelled panels are wider than the real ones. Thus, mass and stiffness of infills need to be suitably adjusted to capture the in-plane behaviour. Usually, the mass density of the modelled infill is reduced in order to obtain the same mass of the real infill; by considering a percentage increment λ of the panel dimensions equal for both sides, the mass density for the modelled element ρ_m can be evaluated as follows

$$\rho_m = \rho/\lambda^2 \tag{5}$$

As for the stiffness, given a constant total mass, the elastic modulus evaluated on the wider panel to fit experimental frequencies of the real infill is overestimated and should be reduced to represent the in-plane stiffness of the infill that, on the contrary, is unaffected by the increment λ of the panel dimensions (if the latter is the same for both directions). For the clamped plate this can be observed directly from Equation (3) that, for the wider panel having mass equal to that of the real infill, provides

$$\tilde{E}_0 = \frac{48\rho_m(1-\nu^2)}{\pi^2 t^2} f_{1,exp}^2 \left[\left(\frac{1+\Delta_{m=1}}{\lambda a}\right)^2 + \left(\frac{1+\Delta_{n=1}}{\lambda b}\right)^2\right]^{-2} \tag{6}$$

By comparing Equations (3) and (6), it results that the equivalent elastic modulus of the wider panel E_m necessary to capture the in-plane behaviour of the real infill should be obtained through

$$E_m = \tilde{E}_0/\lambda^2 \tag{7}$$

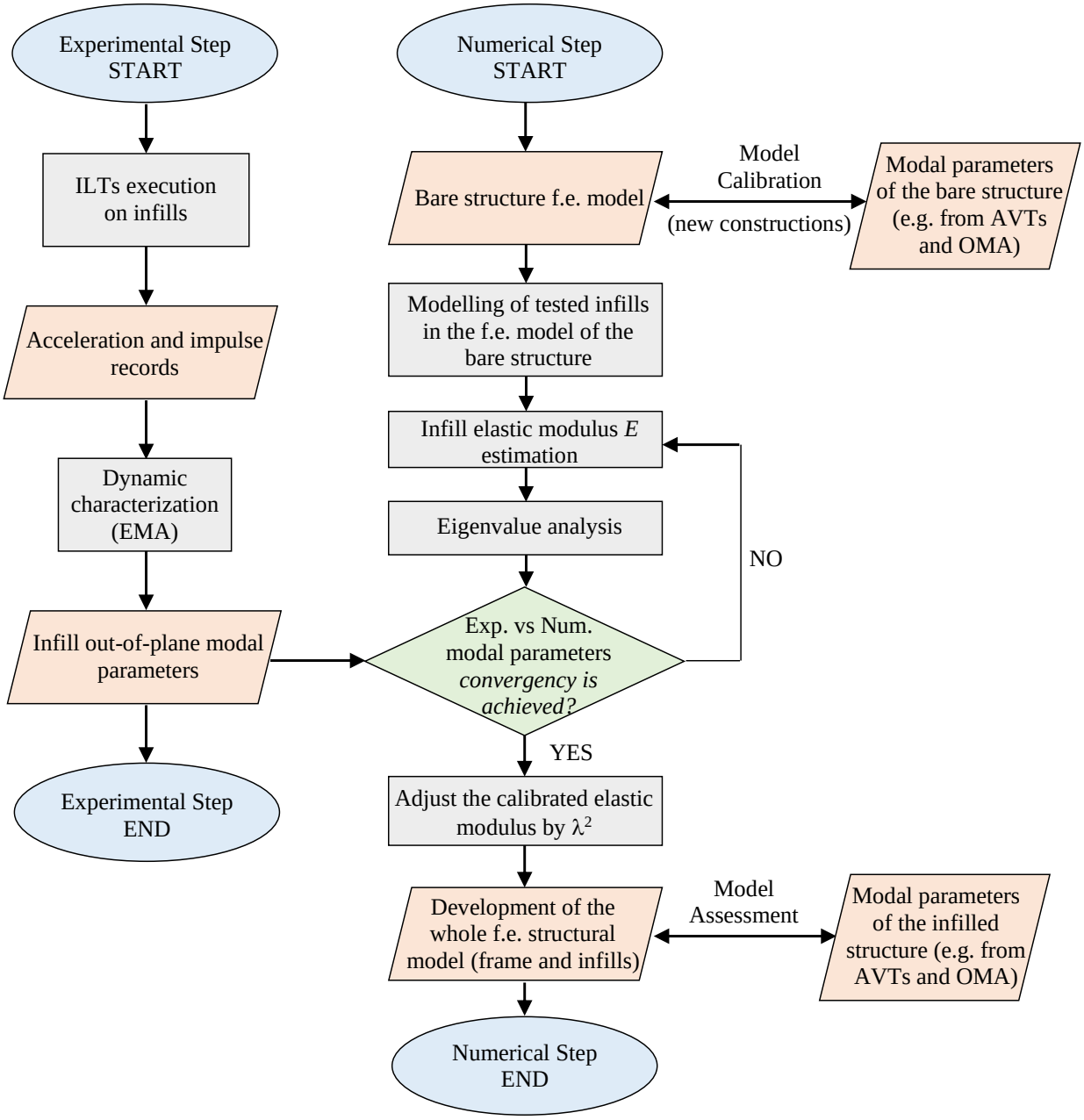

Figure 1. Flow chart of the proposed methodology.

2.3 Final remarks

The masonry infills of the whole structure can be divided in classes characterised by similar geometries (dimensions and thickness) and the proposed methodology can be adopted to estimate the equivalent elastic modulus for all the infill typologies. The estimated elastic moduli are used to develop a numerical f.e. model of the building capable to predict the modal parameters of the whole structure in its operational conditions. In the case of new constructions, although uncertainties in the modelling of the bare structure are generally limited since the geometry of structural members are often known from design and technical drawings and the elastic moduli of construction materials can be evaluated from destructive tests executed for the material acceptance or from in-situ non-destructive tests, the proposed

procedure can take advantage of an experimental dynamic characterization of the bare structure during the building construction. The latter can be achieved by means of AVTs and the Operational Modal Analysis (OMA).

If more refined numerical models of infills are developed, governed by a wider set of mechanical parameters (e.g. orthotropic shell elements are used), the methodology proposed in flow chart of Figure 1 can be used, exploiting sophisticated model updating techniques. However, the use of sophisticated numerical models goes beyond the paper aim, which is that of providing a practical tool for engineers considering conventional modelling strategies. In the following sections, it will be shown that the proposed methodology allows the calibration of structural f.e. models that can accurately predict the dynamic behaviour of the real structure in its operational condition, evaluated through OMA starting from data of AVTs. Consequently, sophisticated models appear not necessary, and the proposed methodology configures as a little invasive, fast and efficient approach for calibrating a f.e. model able to reproduce results of AVTs. Finally, the calibrated f.e. structural model obtained with the proposed methodology can be adopted for nonlinear performance assessments by implementing elastic thresholds of the structural members, allowing for a reliable estimation of the interaction between structural and non-structural members.

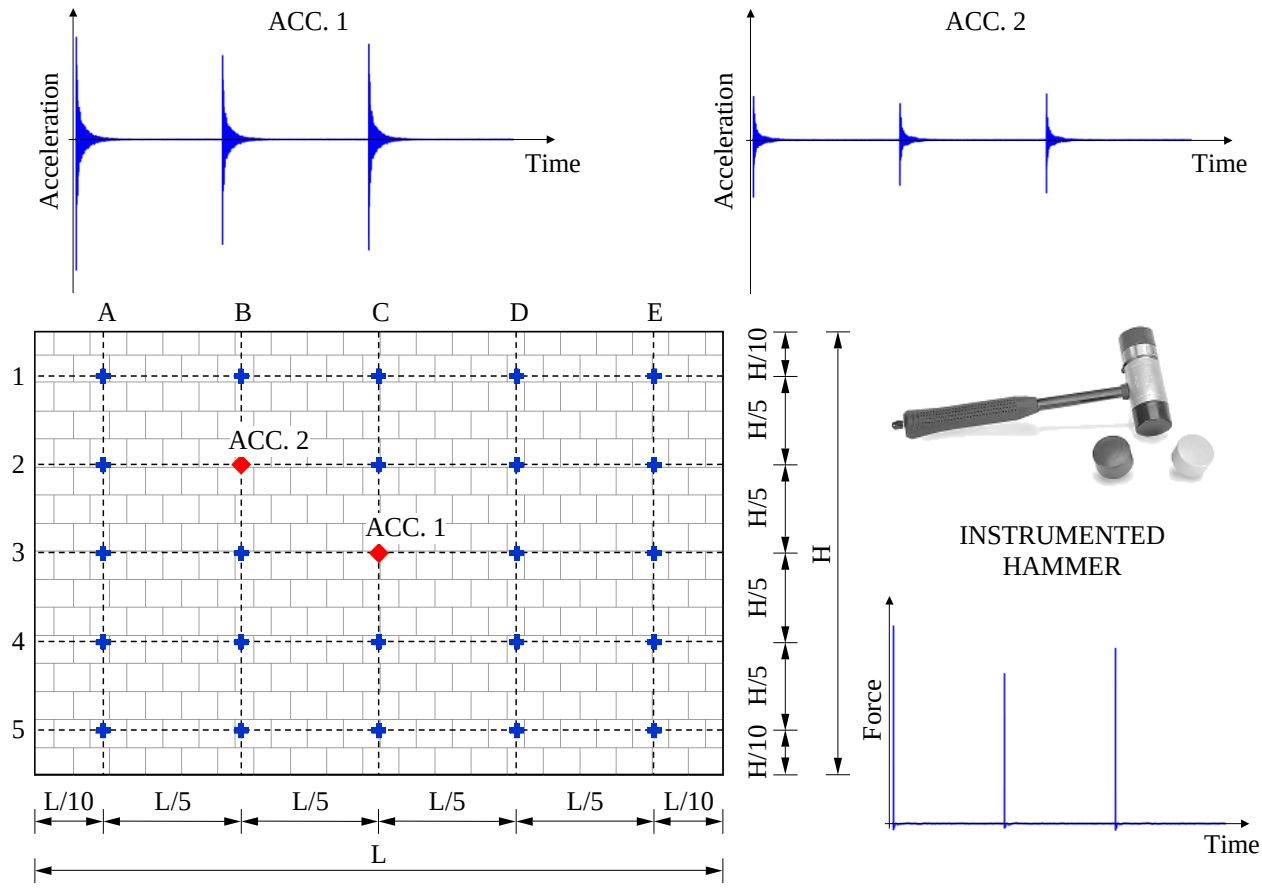

Figure 2. ILTs on infill masonry wall: measurement grid and recorded signals.

3 Validation of the proposed methodology

The basic idea of the proposed methodology is herein validated through laboratory tests in which geometric and mechanical uncertainties in the structural modelling are controlled and mitigated. In detail, a laboratory mock-up is experimentally and numerically investigated to validate the proposed methodology; tests include a thorough dynamic characterization of the mock-up with and without the presence of masonry infills, as well as the test results interpretation through refined f.e. models. Tests relevant to the infilled structure are repeated before and after plastering, in order to (*i*) evaluate the contribution of the plaster that is expected to homogenise the infill behaviour and (*ii*) to "double" the case study for the validation of the procedure. A synthesis of the performed dynamic tests is provided in Table 1.

Table 1. Synthesis of the performed dynamic tests on the laboratory mock-up.

Structural Configuration	Tests on the mock-up	Tests on infills
Phase 1 (P1): Bare frame	ILTs AVTs	---
Phase 2 (P2): Mock-up with infills (without plaster)	ILTs AVTs	ILTs
Phase 3 (P3): Mock-up with infills (with plaster)	ILTs AVTs	ILTs

3.1 Description of the laboratory mock-up

The laboratory mock-up shown in Figure 3d is adopted for the validation of the methodology presented in Section 2. The case study is a steel-concrete composite structure composed by a one-storey two-bay moment-resisting frame with height of 3.00 m and span length of 4.20 m (Figure 3a). Columns are realized with HE160A hot rolled profiles of steel grade S355 and are fixed on the laboratory strong floor by means of four post-tensioned anchor bolts. Beams are made with HE160A hot rolled profiles of steel grade S355; beam-column joints are designed to have a moment resisting frame in the longitudinal direction (2 bays) and a braced frame in the transverse one (1 bay), where horizontal forces are entrusted by X-braces (Figure 3b). The composite deck is obtained with 0.12 m thick C30/37 r.c. slab casted on a collaborating EGB210 steel sheet, connected to beams by means of Nelson studs. One longitudinal and two transverse post-tensioned beams are organised within the slab. The slab post-tensioning allows the applications of both compression and tensile forces at the slab level (i.e. during cyclic load tests on the mock-up) avoiding the slab cracking. To simulate the presence of non-structural and imposed loads, nine 20 cm thick concrete blocks are added over the slab with the arrangement shown in Figure 3c. A ready-mix concrete was used for the blocks that were cast outside the laboratory; the concrete mass density, determined through laboratory tests on cubic specimens collected during the block casting, is about 24 kN/m^3.

After the execution of tests scheduled on the bare structure, two light infill masonry walls (W1 and W2 in Figures 4a and 4c) are built filling only one bay for each longitudinal frame.

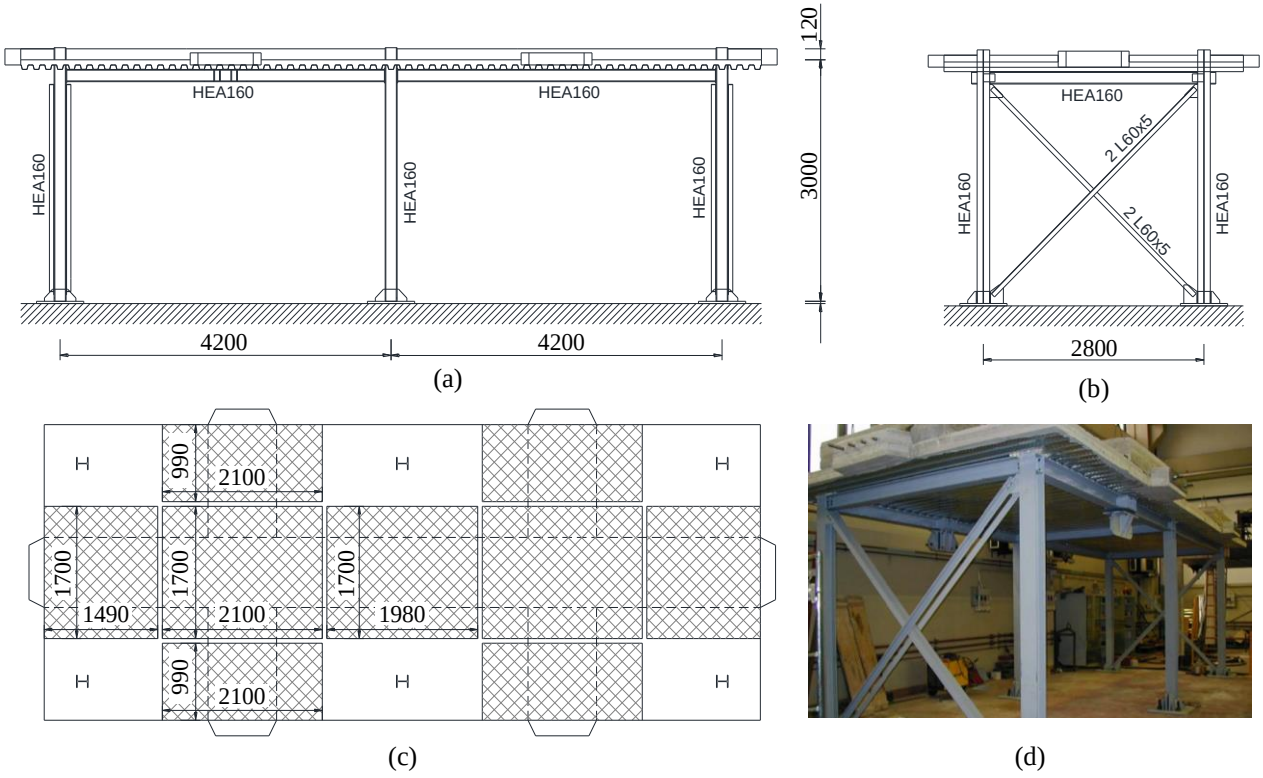

Figure 3. Laboratory mock-up: (a) longitudinal scheme, (b) transverse scheme, (c) additional concrete blocks, (d) general view.

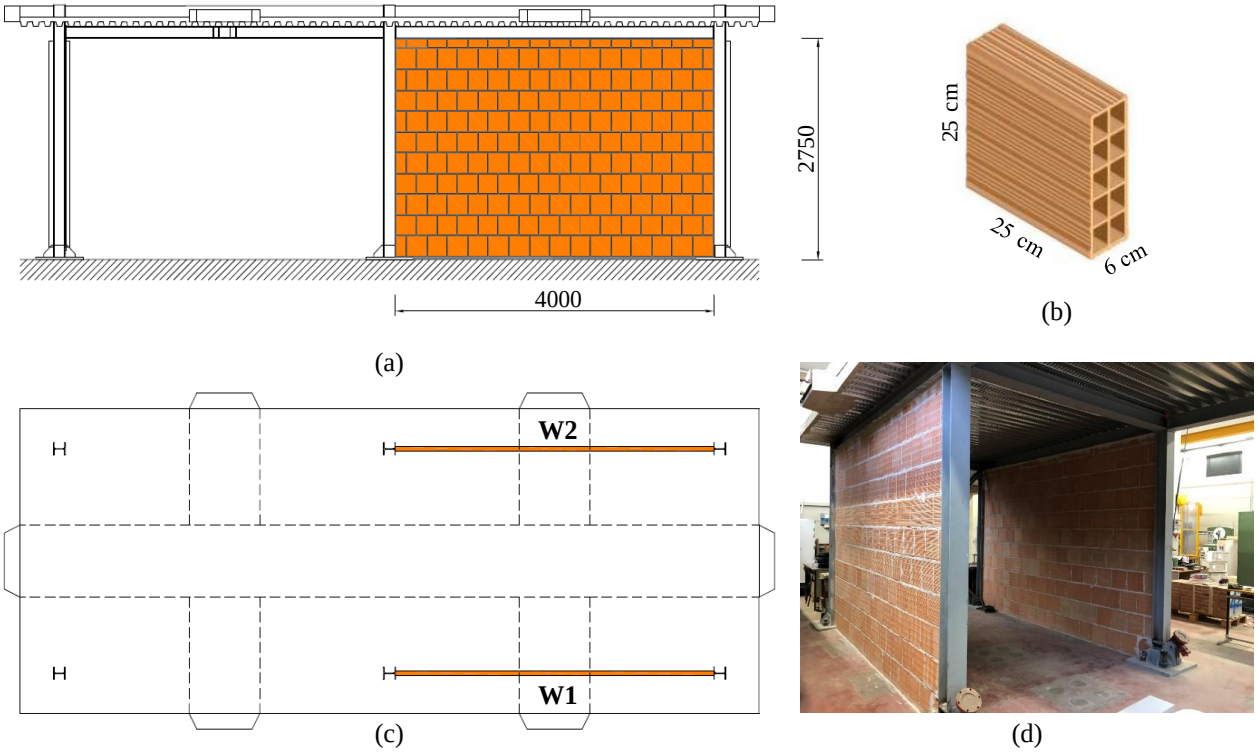

Figure 4. Infilled frame: (a) longitudinal scheme, (b) adopted hollow clay brick, (c) infill wall plan disposition, (d) general view before plaster.

The infills have length of 4.00 m and height of 2.75 m and are made by 25 x 25 cm hollow clay bricks with thickness of 6 cm (Figure 4b), connected to each other by about 1-1.5 cm thick bed joints and by head joints with variable thickness. Walls can be considered as representative of a light infill typology, largely adopted to realize internal partitions in framed buildings. Starting from the construction material typologies and quantities, the infill mass density was computed with a good accuracy and assumed to be 0.918 t/m^3. At the end of tests scheduled on the whole structure and on the infills without plaster, the two walls are covered with a gypsum plaster layer in each side, with thickness of about 0.7 cm, obtaining a 7.4 cm thick panel. The computed infill mass density in this case is 1.192 t/m^3, resulting from the weight of the gypsum plaster, evaluated from dedicated specimens. A view of the infilled mock-up is reported in Figure 4d.

3.2 Dynamic characterization of the mock-up

In this section, tests for the *"Model Calibration"* and *"Model Assessment"* foresee in the flow chart of Figure 1 (Numerical Step) are presented. Results, in terms of modal parameters will be adopted in the following sections for the validation of the proposed procedure.

The experimental modal parameters (i.e. resonant frequencies and mode shapes) of the mock-up are determined through the OMA and the Experimental Modal Analysis (EMA) based on the acceleration measurements of the frame subjected to AVTs and ILTs, respectively. Two different kind of tests and modal analyses are adopted in order to improve the reliability of the results. For AVTs, the input is given by the surrounding environment, namely the vibration due to human activities and ground microtremors, and it is characterized by very low level of excitation to the structure, both in terms of accelerations and displacements. For ILTs the input is given by hammer blows on the structure, hence, the intensity of excitation is slightly higher than for AVTs. As already mentioned, dynamic tests on the mock-up are performed in three phases, corresponding to different structural configurations: (*i*) on the bare frame (P1), (*ii*) after the construction of the infill walls (P2), and (*iii*) after plastering the infills (P3).

The instrumentation adopted to perform the dynamic tests consists in six low-noise uniaxial piezoelectric accelerometers with sensitivity of 10 V/g, frequency range of 0.07 – 300 Hz, and 1 μg of resolution. Sensors are connected to a 24-bit data acquisition system by means of coaxial cables. A laptop equipped with a handmade software developed in LabView [47] environment is used to store data automatically during the tests and to plot the frequency spectra of the recorded accelerations. Furthermore, for ILTs, an instrumented hammer characterized by sensitivity of 0.23 mV/N, measurement range ± 22240 N (peak) and mass of about 1 kg, is used; the hammer, equipped with a soft tip, revealed to be able to investigate frequency range up to 300 Hz. For AVTs, 20 minutes long records sampled at a rate of 2048 Hz are acquired. This time length provides enough data to obtain modal

parameters with a good accuracy [48]. For ILTs, 50 seconds long records sampled at a rate of 2048 Hz are acquired for each hammer blow. This time length ensures to get results with high resolution in the frequency domain. The six accelerometers are positioned on the composite slab according to the layout of Figure 5a that allows the identification of the 3-D dynamic behaviour of the frame, including possible in-plane floor deflections triggered by the aspect ratio of the floor (characterised by a slender rectangular shape). The hammer blows are applied in a corner of the composite slab (point I in Figure 5a) to excite both translational and torsional modes of the mock-up; three hammer blows are applied in order to obtain signals redundancy that allows the computation of more stable and reliable values of the resonant frequencies. In Figure 5b two photos relevant to the sensor array and the impact test execution are shown.

Starting from acceleration measurements of AVTs, the OMA is performed to identify the modal parameters of the mock-up, according to the Covariance-driven Stochastic Subspace Identification (SSI-COV) output-only technique, which is a well-known time domain subspace identification technique that exploits covariance functions of raw output acceleration time histories to formulate the Hankel matrix from which the state transition matrix is obtained through a singular value decomposition. The modal parameters are finally obtained by means of an eigenvalue decomposition of the transition matrix [49]. As for ILTs, modal parameters are identified through the EMA, adopting the Numerical algorithm for Subspace State Space System IDentification (N4SID), that is an input-output technique working in time domain that foresees the evaluation of the oblique projection of the input/output data arranged in Hankel matrices. The singular value decomposition of the oblique projection is then performed to compute state transition matrix [50].

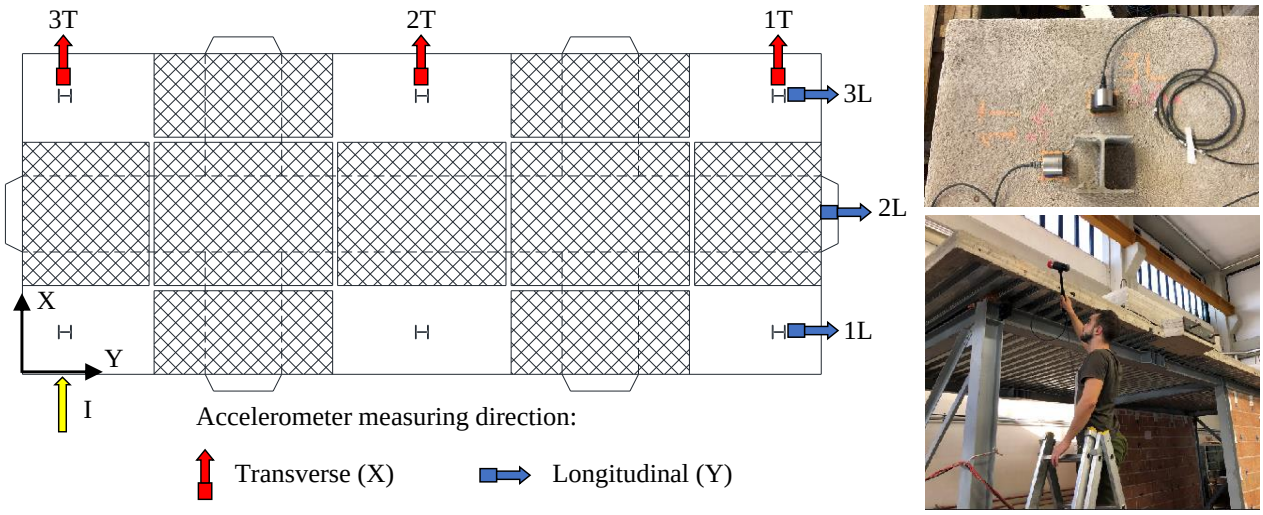

Figure 5. Mock-up dynamic test set up: (a) sensor array, (b) accelerometers in position 1T and 3L (upper photo) and ILT execution (lower photo).

Figure 6 shows the identified vibration modes from OMA and EMA relevant to P1, P2 and P3. With reference to P1, the first two modes are translational in the longitudinal and transverse directions, respectively, while the third one is rotational. After the infill construction (P2) and after plastering (P3), the transverse vibration mode remains almost the same, both in terms of frequency and mode shape since, as expected, the infill stiffness contribution in the transverse direction is negligible. More in detail, a slight decrease of the frequency value is observed for this mode from P1 to P3, probably due to the mass increase, in conjunction with the almost null increase of stiffness. On the contrary, frequency values of the longitudinal and rotational modes increase sensibly passing from P1 to P2 and to P3. In detail, for the longitudinal mode, the increase from P1 to P2 is very high (more than five times) due to the great contribution in stiffness added by infills in the longitudinal direction. After plastering (P3), the longitudinal and rotational modes further increase their frequencies with respect to P2 (around 8% and 5% for the longitudinal and the rotational ones, respectively). It is worth noting that, differently from P1, the longitudinal vibration mode shapes for P2 and P3 present also a slight rotational component, obviously due to the lack of symmetry of the two infills.

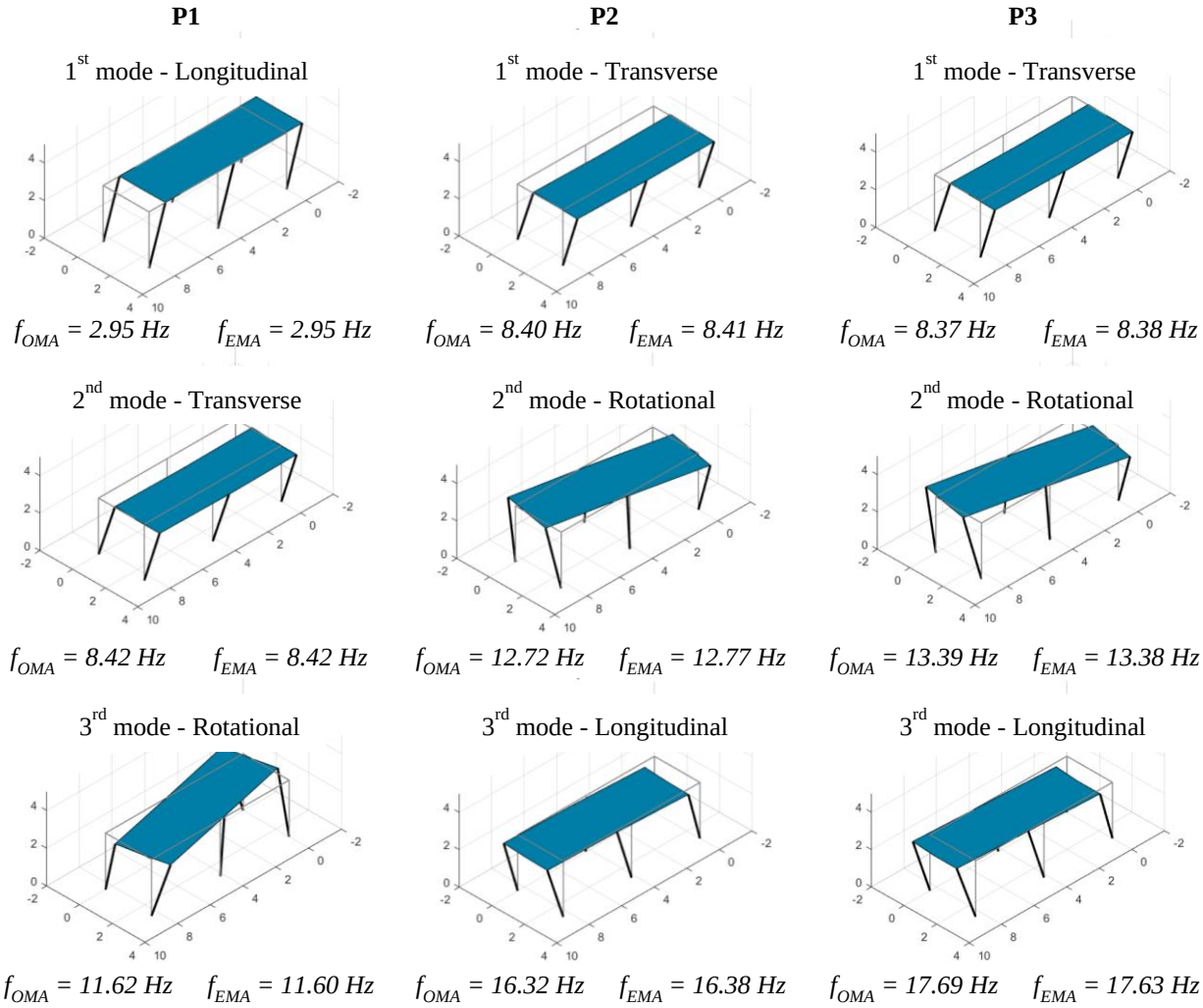

Figure 6. Identified experimental modal parameters of the mock-up at the three phases P1, P2 and P3.

Moreover, frequency values obtained from OMA and EMA for each phase are in very good agreement, proving the results reliability. It is worth observing that the source of excitation for the AVTs, exclusively coming from the laboratory strong floor (e.g. micro-tremors, traffic induced vibrations), is enough to suitably excite the mock-up.

3.3 Dynamic characterization of the out-of-plane response of infill masonry walls

In this section, tasks of the Experimental Step described in the flow chart of Figure 1 are addressed. The infill masonry walls are dynamically tested through ILTs with the aim of identifying the modal parameters of their out-of-plane response. The hammer is the same adopted for the dynamic tests on the mock-up while the accelerations are registered with two uniaxial shear piezoelectric accelerometers with sensitivity of 0.3 V/g and frequency range of 1 – 2000 Hz. Both the hammer and the accelerometers are connected to a 24-bit data acquisition system with chassis, by means of coaxial cables. The acquisition system is connected with a laptop equipped with a LabView software capable to store the recorded data. The test procedures suggested in Section 2 are herein adopted: in detail, sensors are placed as in Figure 2, and dynamic tests consist in providing at least three hammer blows at each of the twenty-five grid points traced on the infill, and in keeping constant the accelerometer positions. For each impact, 10 s long records sampled at a rate of 5120 Hz are acquired. This time length is adequate to obtain results with high resolution in the frequency domain. Since the overall structural dynamic characterization highlights differences in the behaviour of the two infills, ILTs are performed on both walls (W1 and W2), before (P2) and after (P3) the plastering (Figure 7), in order to better investigate the effects of plaster on the dynamic behaviour of the infills and the effectiveness of the proposed procedure.

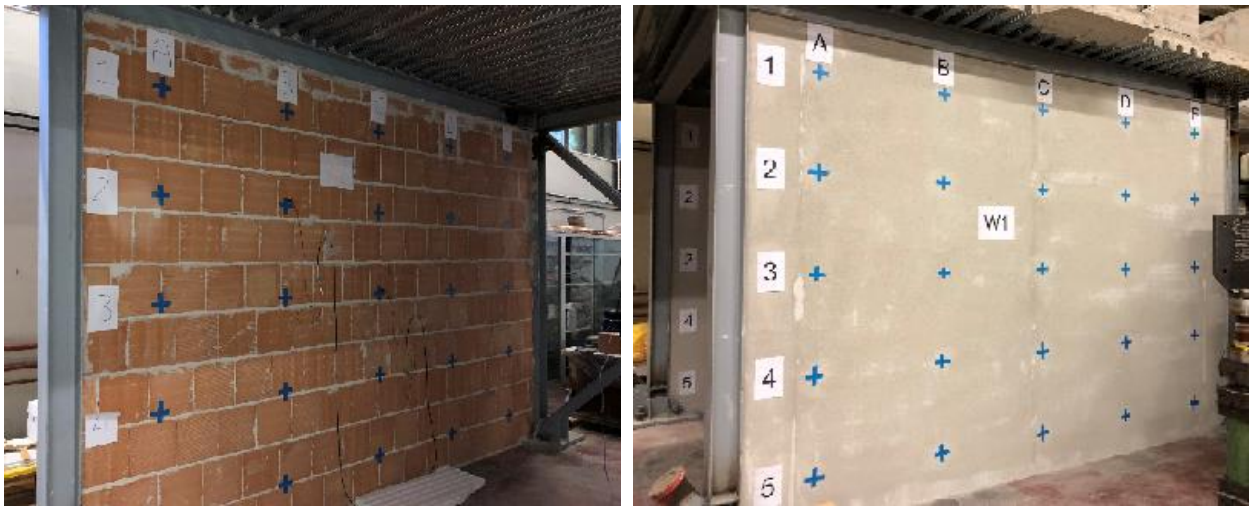

(a) (b)

Figure 7. ILTs on infill masonry walls: (a) W2 before the plaster (P2), (b) W1 after the plaster (P3).

The identified experimental modal parameters are the resonant frequencies and the relevant mode shapes that characterize the out-of-plane dynamic behaviour of the walls. Initially, the Frequency Response Functions (FRFs) for each impact and for each accelerometer are computed to investigate the system response in the frequency domain. As an example, Figure 8 shows the FRFs relevant to impacts in A1, B2 and C3 grid points of both W1 and W2. For each graph, the blue line represents the FRF computed on the basis of the records from ACC1, while the red one refers to records from ACC2. It is worth noting from all diagrams that the two lines present roughly the same peaks, often with different amplitude, demonstrating the usefulness of measuring the output (accelerations) in different locations. Moreover, comparisons of FRFs relevant to the three grid points reveal that some peaks are not present in all of them; this happens when the hammer blow is provided in the correspondence of a nodal line of the mode shapes associated to those missing frequency peaks. Based on this, it is evident the importance to provide inputs in several infill points to get a complete dynamic characterization. Finally, although, as already mentioned, walls generate a non-perfect symmetrical modal behaviour of the infilled frame, the FRFs of the two walls appear very similar. In Table 2, the identified resonant frequency values for both walls are listed. Each vibration mode is named with a couple of number (*n*,*m*) which represent the number of semi-waves present in the mode shape along the horizontal and vertical directions, respectively. First, it is possible to observe that for both the infills a significant number of modes have been identified for both P2 and P3 (twelve modes for P2 and thirteen modes for P3). Experimental data highlight that infills with plaster are characterised by a clearer dynamic behaviour, which overall appear more compliant with that expected for a homogeneous plate.

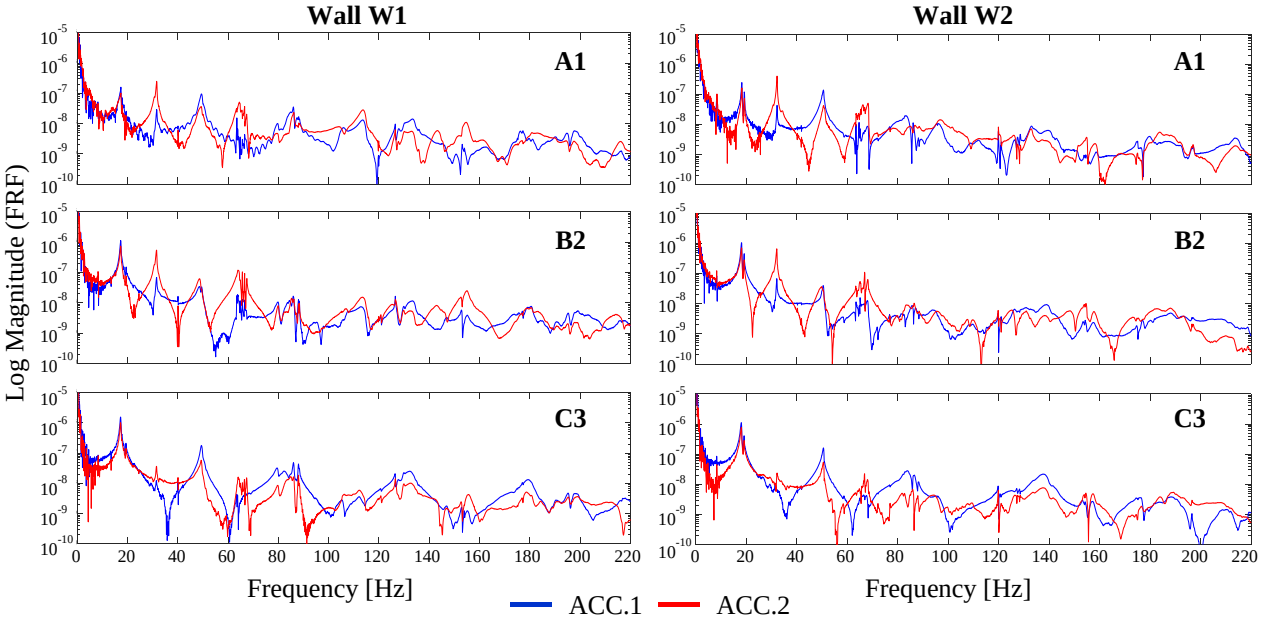

Figure 8. FRFs obtained from three impact point (A1, B2 and C3) for both tested walls.

Table 2. Experimental resonant frequencies for the tested walls without (P2) and with (P3) plaster.

Mode name	Frequency [Hz]			
	W1		W2	
	P2	P3	P2	P3
1,1	16.80	17.30	17.90	18.10
2,1	27.47	31.60	29.53	32.15
1,2	40.10	49.00	48.00	49.97
3,1	46.55	49.40	45.35	50.50
2,2	57.54	63.88	59.20	64.50
4,1	63.07	66.50	66.85	68.10
5,1	76.85	120.71	78.93	119.90
3,2	79.79	85.98	76.10	82.67
2,3	/	105.30	/	107.13
4,2	104.98	113.75	104.40	127.30
3,3	117.77	131.19	119.40	133.20
5,2	132.28	143.93	139.10	155.90
5,3	177.60	198.85	175.24	212.50

By comparing frequency values obtained from P2 and P3, a general increase emerges which depends on the mode and is in the range between 2% and 22% (with a mean value of about 14%), excepting for mode *5,1*, for which an increase of about 60% is observed, passing from about 76 Hz to about 120 Hz for both the walls. Furthermore, comparing frequencies of the two walls relevant to P2, it is possible to observe that values relevant to W1 are slightly lower that W2 (of about 4%), meaning that W1 is less rigid than W2 (being the mass nearly the same). Since the same discrepancies characterise resonant frequencies of W1 and W2 in P3 (frequency values relevant to W1 are around 3% lower than W2), it is possible to conclude that the plaster layer has almost the same features for the two walls and provides very similar contribution, both in terms of mass and stiffness.

Finally, in Figure 9 the mode shapes inherent to all the identified vibration modes of W1 in P3 are shown (those relevant to W2 in P3 are qualitatively the same). They are represented starting from the modal displacements identified for each mode and for each grid point and using a Matlab algorithm [51], which permits to obtain smooth surfaces using a biharmonic spline interpolation method.

3.4 Validation of the proposed methodology for the estimation of the infill elastic modulus

In this section, the reliability of the estimated equivalent elastic modulus through the proposed approach is evaluated comparing numerical predictions of the modal parameters with experimental ones obtained in Section 3.2. According to flow chart of Figure 1, the equivalent elastic moduli of the infill masonry walls are estimated according to the proposed simplified approach based on results of experimental dynamic test with the support of a f.e. model of the whole mock-up developed with a commercial

software [52]. Uncertainties relevant to the modelling of the bare structures affects the infill elastic modulus estimation, since they overall have influence on the infill restraint conditions.

In order to reduce such uncertainties, a refined model of the bare structure is firstly developed (Figure 10) and calibrated to comply with the results of dynamic tests on the bare structure (P1). All steel members are modelled with shell elements to capture their torsional stiffness due to warping, which revealed crucial to properly account for the actual boundary conditions of infill walls (e.g. to capture the interaction between the masonry infills and the steel structural members). Shell elements are also used for the steel-concrete composite slab and the added masses, the latter consisting in concrete blocks placed on the floor.

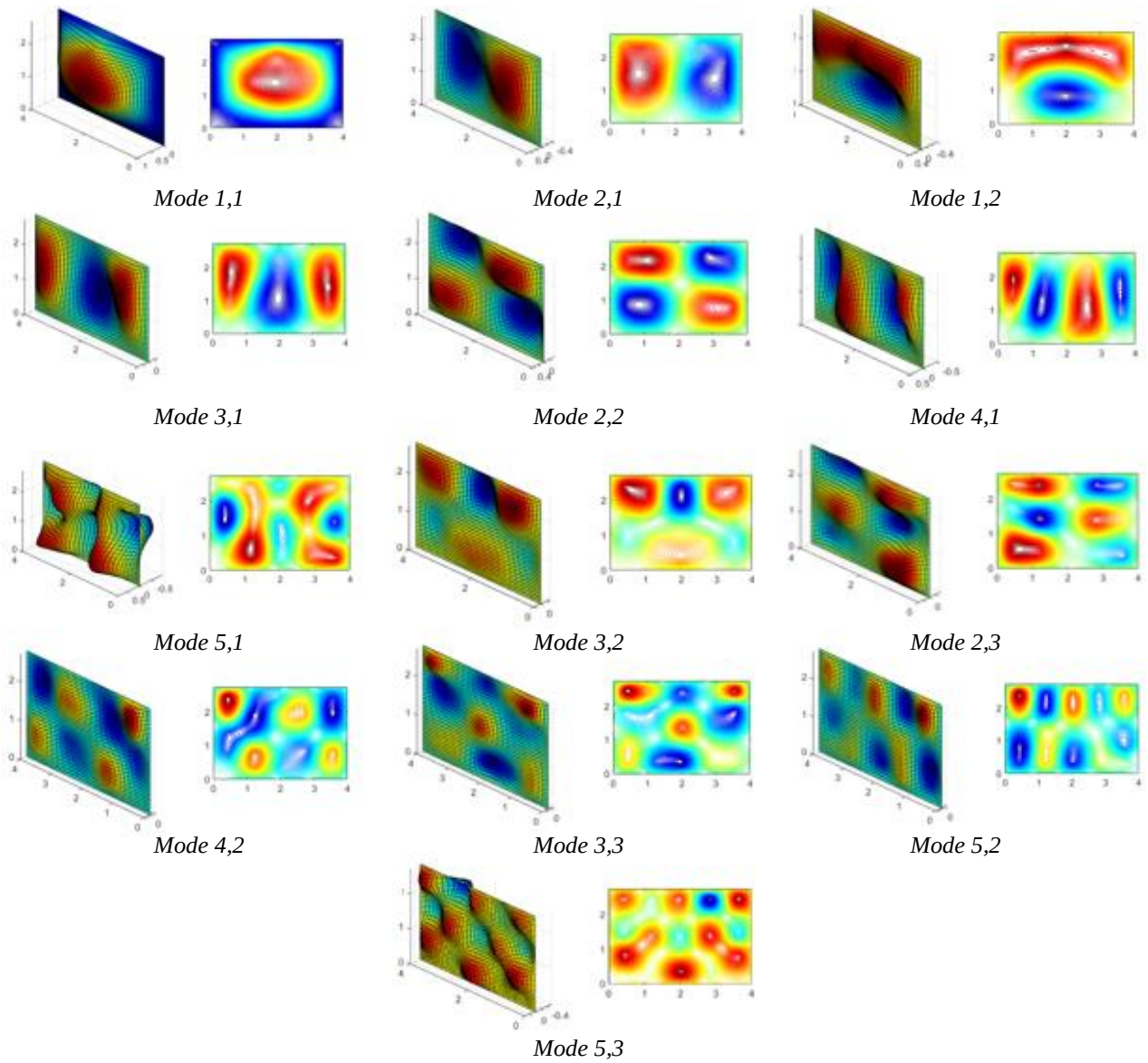

Figure 9. Experimental mode shapes for W1 obtained from P3.

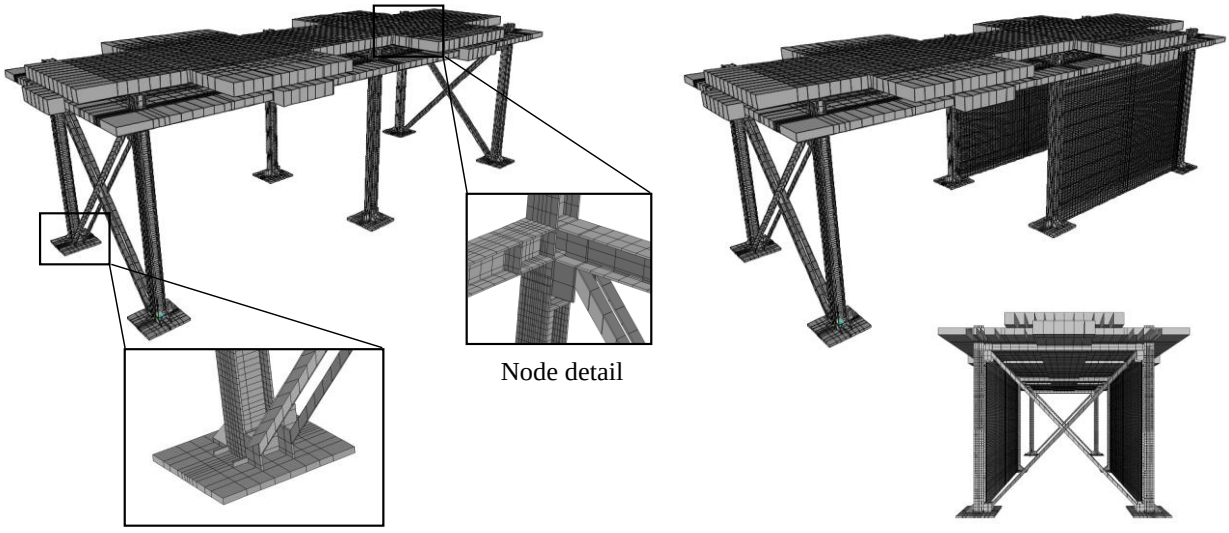

(a) (b)

Figure 10. Mock-up global 3-D f.e. model: (a) bare frame, (b) infilled frame.

The shear connection at the slab level is modelled with elastic links that simulate the stud stiffness embedded in the concrete. Furthermore, all the steel plates constituting the stiffeners of the beam-column and base joints are modelled. Finally, base plates are fixed at the base. The masses are automatically calculated by the software based on the geometry and the mass density of the modelled elements. This model is preliminary calibrated making it capable to predict numerically the experimental dynamic behaviour of the mock-up determined through dynamic tests on the bare frame (P1); with reference to the first three modes, differences between the numerical and experimental frequency values are lower than 1% (column P1 in Table 3) and the MAC values (matrices diagonal entries in Figure 11a) are greater than 0.95.

Both the infill masonry walls are modelled within the frame f.e. model as thin homogeneous isotropic shell elements and are assumed to be clamped at the base edge. Since the aim of the proposed approach is that of calibrating an equivalent elastic modulus for the shell elements, the plaster may be not physically modelled being its contribution considered in the definition of the elastic modulus. However, in this work, two different f.e. models are derived by varying the wall thickness (6 cm for P2 and 7.4 cm for P3) and the wall mass density to simulate the wall conditions without and with plaster (P2 and P3). For each model, the iterative procedure suggested in Figure 1 is performed, varying the elastic modulus E of the infill material and performing modal analyses with Eigen vectors until converge criteria (Equations (4)) are satisfied, assuming δ_f = 5% and δ_s = 25% and considering all the identified modes. In Figure 12 the typical mode shapes for the infills within the frame obtained with the numerical model, are depicted.

Table 3. Experimental and numerical mock-up resonant frequencies at different construction phases.

Mode	Frequency [Hz]								
	P1			P2			P3		
	EXP		NUM	EXP		NUM	EXP		NUM
	OMA	EMA		OMA	EMA		OMA	EMA	
Longitudinal (Y)	2.95	2.95	2.96	16.32	16.38	16.38	17.69	17.63	17.71
Transverse (X)	8.42	8.42	8.40	8.40	8.41	8.40	8.37	8.38	8.38
Rotational	11.62	11.60	11.67	12.72	12.77	12.94	13.39	13.38	13.08

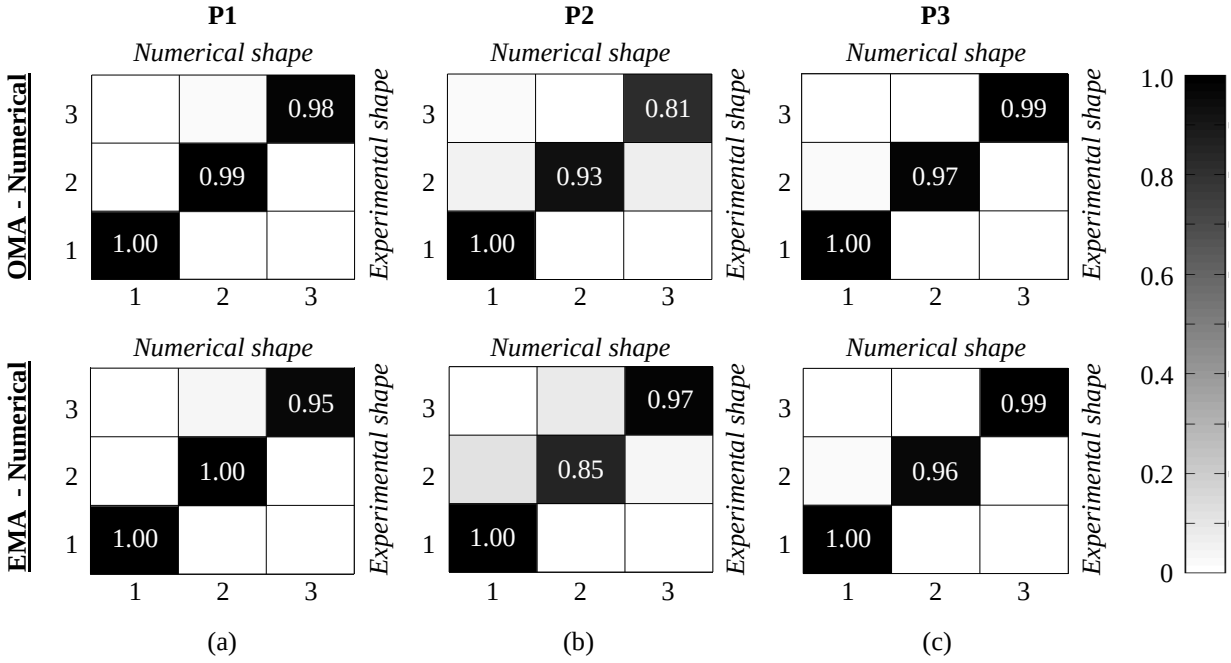

Figure 11. MAC indexes between experimental (OMA and EMA) and numerical mode shapes of the mock-up at different construction phases.

Table 4. Estimated value of E and E_0 for infill walls W1 and W2 and comparison between experimental and numerical modal parameters during P2 and P3.

Mode name	P2						P3					
	W1 E_0 = 2445 MPa **E = 4700 MPa**			W2 E_0 = 2775 MPa **E = 5340 MPa**			W1 E_0 = 2210 MPa **E = 4900 MPa**			W2 E_0 = 2420 MPa **E = 5360 MPa**		
	f_{exp} [Hz]	f_{num} [Hz]	MAC	f_{exp} [Hz]	f_{num} [Hz]	MAC	f_{exp} [Hz]	f_{num} [Hz]	MAC	f_{exp} [Hz]	f_{num} [Hz]	MAC
1,1	16.80	16.38	0.97	17.90	17.31	0.98	17.30	17.42	0.97	18.10	18.18	0.99
2,1	27.47	26.00	0.73	29.53	27.45	0.98	31.60	27.42	0.95	32.15	28.47	0.98
1,2	40.10	44.23	0.51	48.00	46.89	0.64	49.00	47.60	0.88	49.97	49.54	0.71
3,1	46.55	42.71	0.63	45.35	44.81	0.75	49.40	44.20	0.86	50.50	45.77	0.82
2,2	57.54	55.20	0.84	59.20	58.42	0.89	63.88	58.90	0.94	64.50	61.23	0.75
4,1	63.07	62.71	0.63	66.85	65.36	0.81	66.50	63.19	0.91	68.10	64.96	0.80
5,1	76.85	79.48	0.65	78.93	81.32	0.71	120.71	115.16	0.52	119.90	117.42	0.73
3,2	79.79	73.73	0.56	76.10	77.93	0.60	85.98	78.38	0.51	82.67	81.80	0.69
2,3	/	/	/	/	/	/	105.30	103.47	0.75	107.13	106.85	0.74
4,2	104.98	99.45	0.62	104.40	105.03	0.57	113.75	105.69	0.80	127.30	109.70	0.60
3,3	117.77	117.84	0.50	119.40	121.38	0.51	131.19	127.72	0.51	133.20	131.63	0.53
5,2	132.28	131.07	0.71	139.10	138.08	0.55	143.93	138.31	0.57	155.90	142.97	0.52
5,3	177.60	180.39	0.68	175.24	190.30	0.50	198.85	193.44	0.50	212.50	201.43	0.50

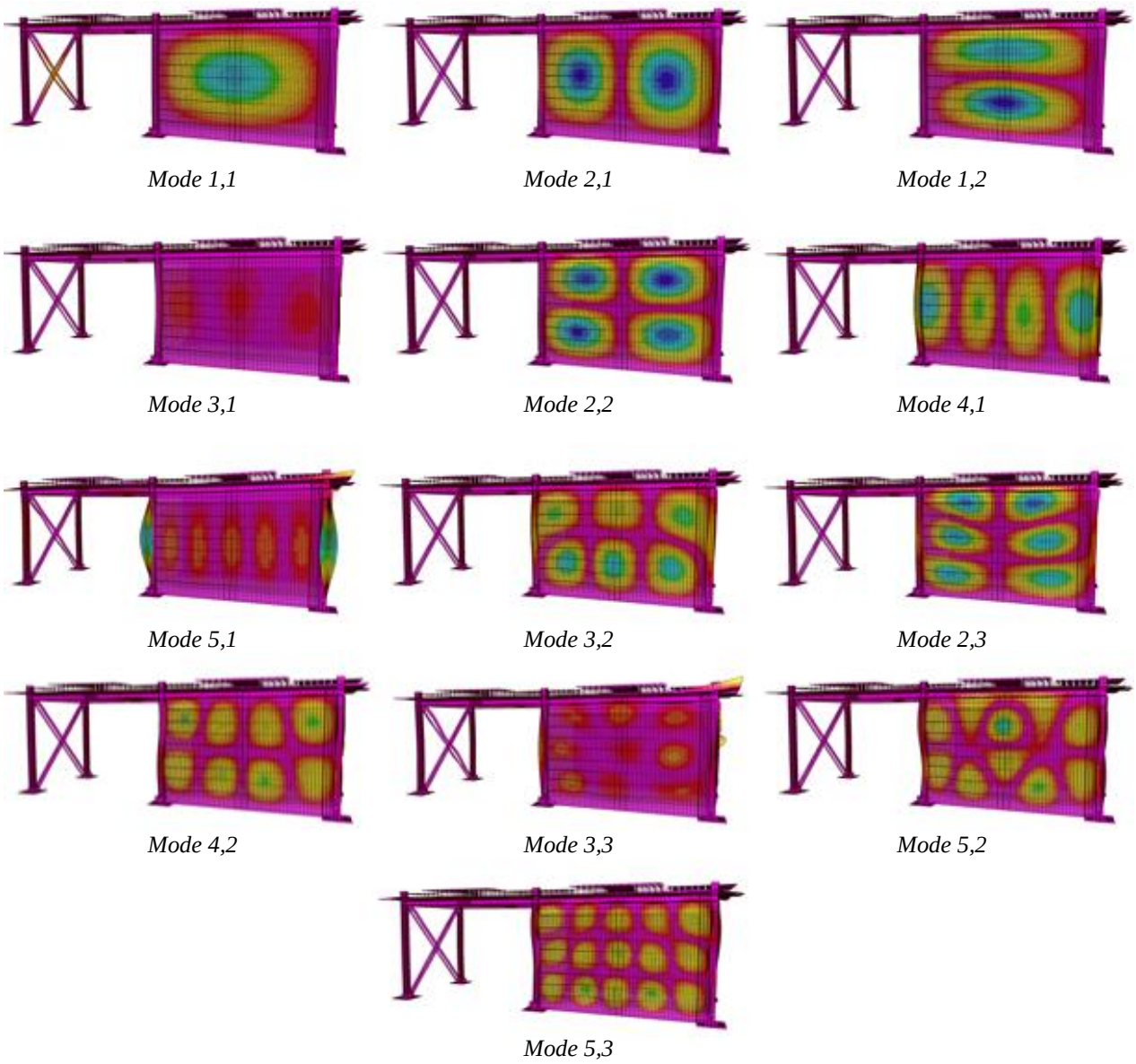

Figure 12. Infill numerical mode shapes within the global 3-D f.e. model.

The obtained equivalent elastic moduli E of the infills and tentative one E_0 are reported in Table 4, together with the comparison between the infill experimental and numerical frequency values and mode shapes, the latter represented by the MAC indexes. As can be observed, the proposed procedure makes it is possible to find an equivalent elastic modulus for the infills (for both W1 and W2 in P2 and P3) that assures a good agreement between numerical and experimental modal parameters for all the identified modes, especially for the infills with plaster. It is worth noting that, in this case, the mass densities and the equivalent elastic moduli have not to be reduced since the modelled infill dimensions are the same of the real ones.

Finally, to verify the reliability of the wall stiffness estimation and the modelling effectiveness on the overall structural dynamic response of the infilled mock-up, the numerical modal parameters of the whole structure are compared with the relevant experimental ones obtained through AVTs and ILTs on

the infilled frame (P2 and P3). In the second part of Table 3 (columns P2 and P3) the numerical resonant frequencies of the first three infilled mock-up vibration modes are reported, and it can be seen that they are in very good agreement with the corresponding experimental ones. The same consideration holds from the observation of the matrices in Figure 11b,c, where the MAC indexes between the numerical and experimental mode shapes indicate a good correspondence between each other, with values greater than 0.81.

4 Application to a real structure

To evaluate the applicability of the proposed methodology with respect to a real structure, which is characterised by significantly higher levels of uncertainties concerning material properties and dimensions with respect to the laboratory mock-up, an application to a full-scale case study is herein presented. In detail, the methodology is applied on an infilled r.c. frame building (Figure 13a), which was experimentally tested during the construction. The structure has a 16.50 x 11.70 m rectangular plan and a total height of 8.00 m (with one storey plus the underground floor and an attic). The ground floor hosts two detached housing units with an almost square plan misaligned in North-South direction (Figure 13b). The structure is composed by spatial r.c. frames above the ground surface, while the underground level is made of r.c. retaining walls with thickness of 0.30 m. The foundation system consists of 10 m deep drilled piles with caps connected by tie beams placed in the transverse and longitudinal directions. The access to the underground level is achieved by two external r.c stairs attached to the East and West sides of the building and by two r.c. garage ramps with lateral r.c. retaining walls separated to the main building. The internal and external infill masonry walls are made with hollow clay bricks with different dimensions and, in some parts, double brick walls are used to improve insulation. The external and internal infills can be divided in three different construction typologies, indicated with labels E1, I1 and I2 (Figure 14). E1 is adopted for all the external walls, which are built only at the ground and at the attic level. The I1 is used for the internal walls dividing the two housing units at the underground and ground level; the I2 is adopted for all the internal partitions. The plan wall distribution can be considered uniform in both the underground and ground floor, while there are no internal infills at the attic floor.

The building was dynamically tested twice: the first experimental campaign consists in an AVT after the construction of the bare structure, while the second one, performed at the end of the infill masonry walls construction (without plaster), consists in an AVT on the overall structure and in ILTs on some infills of each typology.

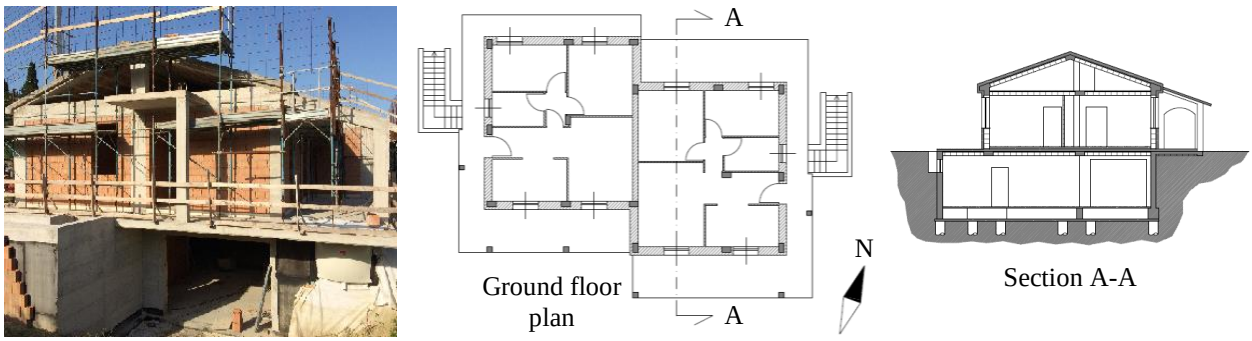

Figure 13. Infilled r.c. frame building case study: (a) general view during construction, (b) ground floor plan and architectural section.

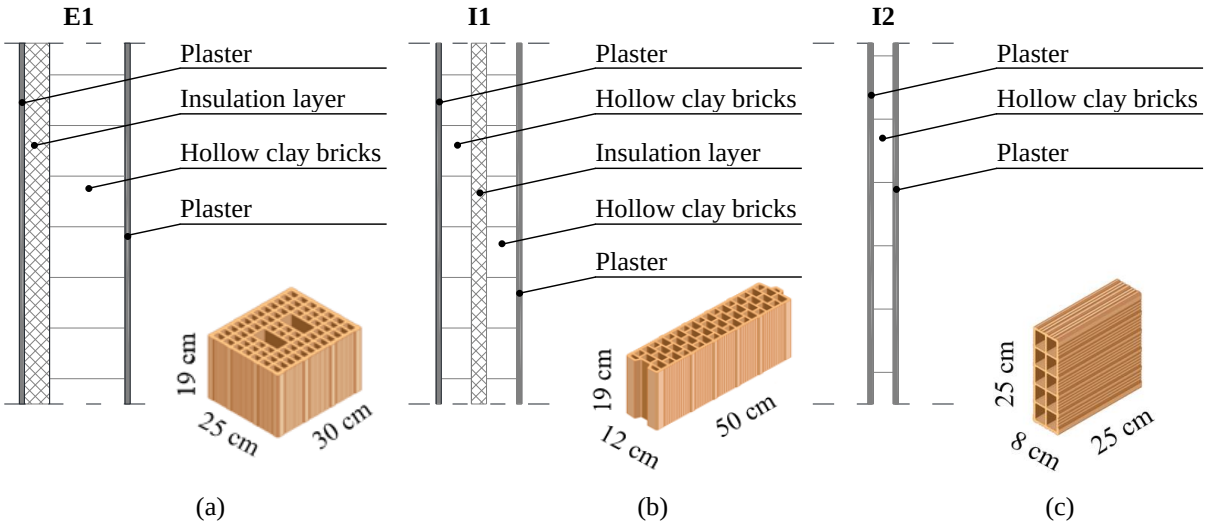

Figure 14. Infill masonry wall typologies: (a) external wall E1, (b) internal wall I1, (c) internal wall I2.

AVTs are performed using low noise uniaxial piezoelectric accelerometers with a wired acquisition system; eight sensors are used, four located at the ground (Figure 15a) and four at the attic floor (at the same position), with the aim of obtaining a dynamic characterization of the overall building. The building modal parameters are obtained through OMA. The ILTs on infills are performed using the same instrumentation, test configurations and methodology described before for the laboratory mock-up, consistently with procedures suggested within the proposed methodology. Three infills are considered and tested (W-E1, W-I1 and W-I2) with the aim of investigating the wall typologies adopted for the external and internal partitions. All the tested walls, located at the ground floor (Figure 15a), have not openings and, in most cases, the head joints are almost completely absent, while the bed joints have about 1-1.5 cm of thickness. W-E1 is an external infill wall built with E1 construction typology (Figure 15b), W-I1 is an internal partition which divides two housing unit, built with I1 typology (Figure 15c) and W-I2 is a typical light interior partition wall built with I2 typology (Figure 15d). The

wall geometry is detailed in Figure 15; it is worth observing that infill W-I1 and W-I2 are not completely confined by the r.c. frame since on one side they are connected to an orthogonal wall. It will be shown in the sequel that the proposed procedure provides satisfactory results also in this case, being the orthogonal wall capable of proving a degree of restraint for the out-of-plane dynamics of W-I1 and W-I2 comparable with the one offered by the frame in the case of small vibrations.

Based on acceleration records of the ILTs, four vibration modes for each panel are identified; the resonant frequencies are reported in Table 5 and the relevant experimental mode shapes are shown in Figure 16.

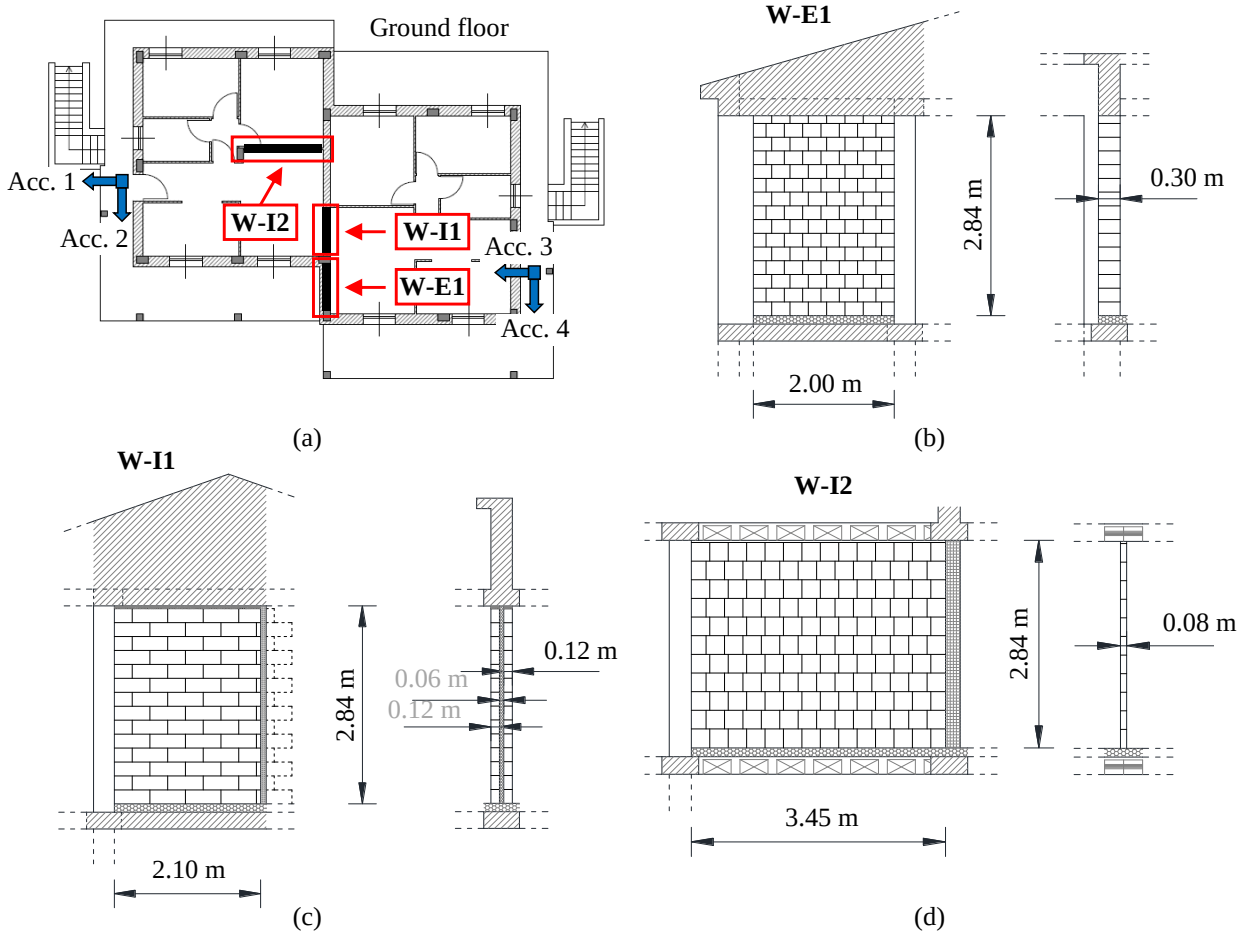

Figure 15. (a) Tested infill masonry walls and sensor placement for AVTs, (b) wall W-E1, (c) wall W-I1, (d) wall W-I2.

Table 5. Experimental resonant frequencies for the building infill masonry walls.

W-E1		W-I1		W-I2	
Mode	f [Hz]	Mode	f [Hz]	Mode	f [Hz]
1,1	64.73	*1,1*	41.81	*1,1*	22.10
1,2	88.93	*1,2*	72.09	*2,1*	40.28
2,1	161.74	*1,3*	122.53	*1,2*	49.88
2,2	201.52	*2,2*	151.56	*2,2*	64.57

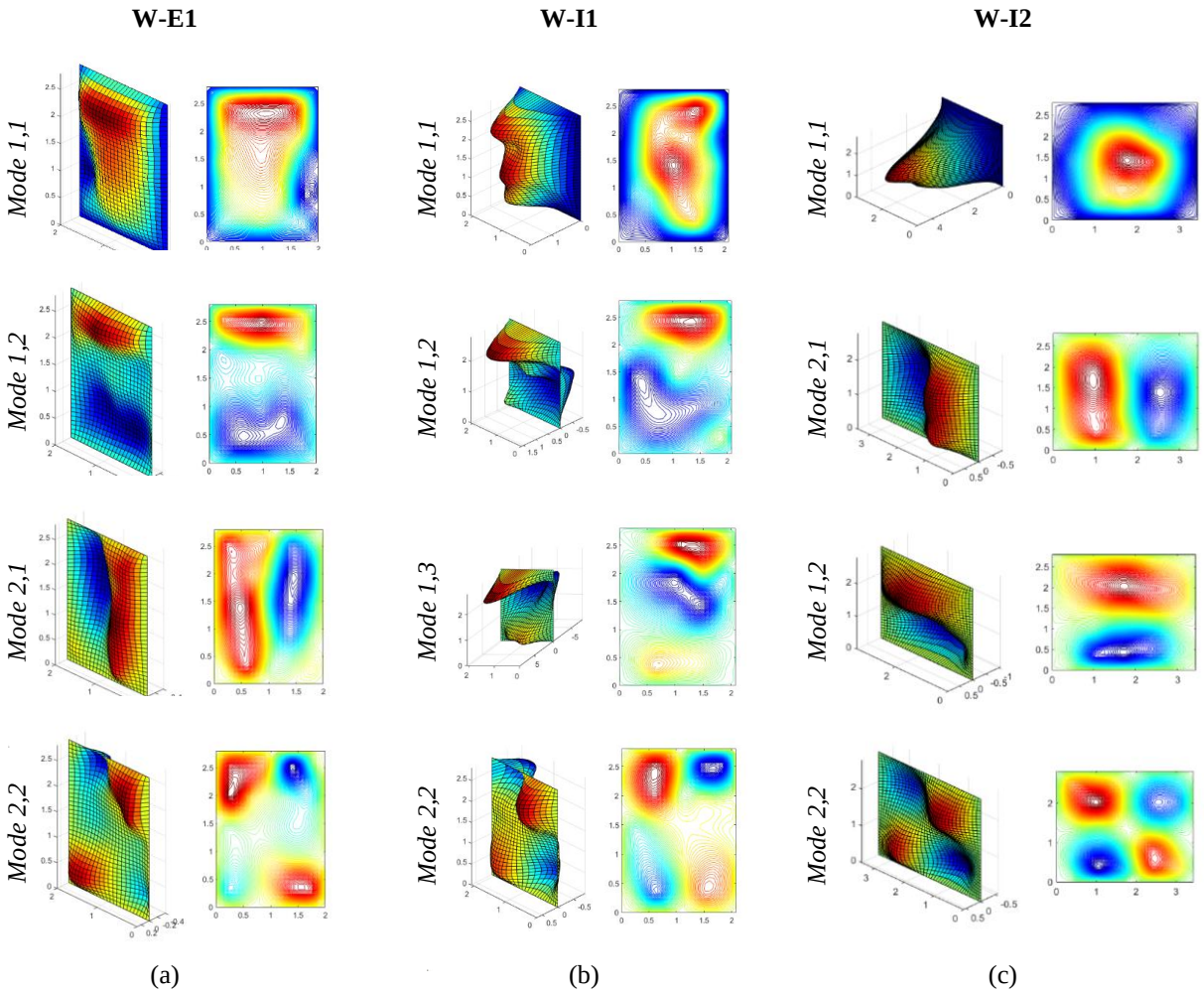

Figure 16. Building infill experimental mode shapes: (a) wall W-E1, (b) wall W-I1, (c) wall W-I2.

According to the proposed methodology, tested infills with their estimated equivalent modulus were included in the 3-D f.e. model of the bare frame developed by means of a commercial software [52]. At first, beams and columns are modelled with elastic frame elements while floors, stair slabs and retaining walls with shell elements; columns and retaining walls are assumed to be fixed at the base. The structural masses are considered automatically by the software. To estimate the dynamic elastic moduli of concrete and, consequently, to reduce the modelling uncertainties, an extensive ultrasonic in-situ campaign was performed. Two beams, eleven columns and three retaining walls were tested to obtain an average concrete elastic modulus for each elevation, that can be representative for the different casting phases. The developed f.e. model of the bare frame revealed capable to reproduce the real dynamic behaviour of the building, identified through results of AVT on the structure without infills, with good accuracy. Indeed, as reported in the first two columns of Table 6, the numerical resonant frequencies relevant to the bare structure are very close to the experimental ones and the same can be concluded for

the mode shapes, since the MAC indexes (Figure 17a), calculated between experimental and numerical mode shapes, are very close to one.

Then, tested infills are included in the f.e. model with shell elements; in order to model as accurately as possible the boundary conditions of the panels, infills in the direct nearby of the tested ones are included with their relevant properties, depending on the typology to which they belong. To estimate the equivalent elastic modulus of each infill, an iterative procedure is performed for each tested wall (three iterative procedures are thus developed). During the first iterative procedure (i.e. for the calibration of the first infill typology) only the elastic modulus of the tested infill is iteratively adjusted by maintaining the initial tentative one for all the others included in the modelling; Equation (3) is adopted to this purpose. This pragmatic approach is suggested to make the proposed approach feasible, starting from the consideration (observed numerically) that the restraint conditions provided by adjacent panels to the investigated one is not very sensitive to the variation of the elastic modulus of the confining panels. Once the equivalent elastic modulus is obtained for an infill typology, this can be used in the iterative procedures performed to calibrate the elastic modulus of the remaining infill typologies. As before, the used convergence criteria are δ_f = 5% and δ_s = 25%, which allow a sufficient accuracy of the results, as will be demonstrated hereafter. Differently from the laboratory mock-up, in this case columns and beams are classically modelled with frame elements (as usual in the practice), so that the dimensions of the modelled infill panels are greater than the real ones. Hence, the mass densities and the estimated equivalent elastic moduli are suitably reduced as proposed in Section 2. For the sake of simplicity, the mean percentage increment λ of the infill dimensions is considered for each panel.

The proposed methodology provides the results reported in Table 7 for the equivalent elastic modulus of the infill typologies. Table 7 also compares experimental and numerical modal parameters for each wall. The infilled global f.e. model obtained at the end of the procedures for the elastic modulus estimation is capable to represent the dynamic behaviour of the real building; in fact, as already mentioned for the bare structure, the numerical modal parameters, obtained with the f.e. model, are in good agreement with the experimental ones, as reported in the last two columns of Table 6 and in Figure 17b.

Table 6. Experimental and numerical resonant frequencies for the building.

Mode	Mode typology	Frequency [Hz]			
		Bare structure		Infilled structure	
		EXP	NUM	EXP	NUM
1st	Translational North-South	5.77	5.76	10.71	10.74
2nd	Roto-translational East-West	6.12	6.24	13.04	13.09
3rd	Rotational	7.85	7.68	15.75	14.94

Table 7. Estimated in-situ wall E and E_0 and comparison between experimental and numerical modal parameters.

W-E1 E_0 = 400 MPa **E = 3000 MPa**				W-I1 E_0 = 1070 MPa **E = 2550 MPa**				W-I2 E_0 = 1650 MPa **E = 3150 MPa**			
Mode name	f_{Exp} [Hz]	f_{Num} [Hz]	MAC	Mode name	f_{Exp} [Hz]	f_{Num} [Hz]	MAC	Mode name	f_{Exp} [Hz]	f_{Num} [Hz]	MAC
1,1	64.73	61.49	0.82	*1,1*	41.81	40.85	0.91	*1,1*	22.10	21.97	0.98
1,2	88.93	87.70	0.72	*1,2*	72.09	72.51	0.50	*2,1*	40.28	41.57	0.96
2,1	161.74	169.68	0.75	*1,3*	122.53	121.74	0.90	*1,2*	49.88	46.89	0.50
2,2	201.52	219.99	0.50	*2,2*	151.56	145.23	0.65	*2,2*	64.57	63.77	0.85

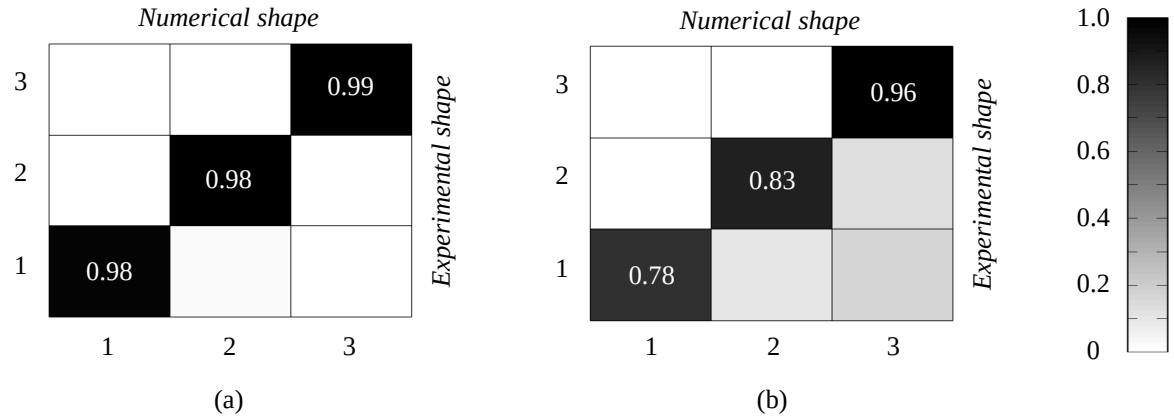

Figure 17. MAC indexes between experimental and numerical building mode shapes: (a) bare structure, (b) infilled building.

5 Conclusions

In this paper an expeditious procedure to estimate the stiffness of masonry internal partitions and infill walls is proposed with the aim of providing a practical tool to reduce uncertainties in the f.e. modelling of frame buildings when partitions and infills must be included. This is fundamental when a refined model of the structure, including both structural and non-structural components, is necessary to interpret results of ambient vibration tests or for the design of particular seismic retrofitting systems that require the structural operativity after severe earthquakes. The proposed methodology foresees the execution of dynamic impact load tests on infills from which the modal parameters of the out-of-plane response of the masonry panel are identified. Experimental modal parameters of infills are used to estimate an equivalent elastic modulus which can be adopted in a conventional 3-D f.e. modelling in which infills are schematised as elastic homogenous isotropic shell elements.

The main remarks of the proposed expeditious methodology can be summarised as follows:

- tests are fast and non-invasive so that they can be easily and widely executed on existing structures;
- masonry infills can be divided in classes characterised by similar geometries (dimensions and thickness) and construction typologies, in order to reduce the number of tests;
- sophisticated numerical models for infills are not required and conventional approaches for modelling r.c. frames and infills, based on beam and shell elements, can be adopted;
- the procedure revealed effective when applied to a real infilled r.c. frame structure, leading to the development of a numerical model able to predict resonance frequencies with errors lower than 1% for translational modes and 5% for torsional ones (with respect to experimental values).

Finally, the procedure configures as a simple and efficient tool, which can be also employed by engineers in the practice, to get a reliable estimation of the elastic mechanical parameters for infill masonry walls and partitions; the procedure improves the one usually adopted, consisting on the calibration of the infill stiffness through a trial and error approach based on the convergence of numerical and experimental modal parameters from ambient vibration tests on the whole building. In this sense, main advantages of the proposed approach can be appreciated for buildings with different infill masonry wall typologies.

References

[1] Asteris P.G. Lateral stiffness of brick masonry infilled plane frames. J. Struct. Eng., 129, 1071-1079, 2003.

[2] Cavaleri L., Fossetti M., Papia M. Infilled frames: developments in the evaluation of cyclic behaviour under lateral loads. Struct. Eng. Mechanics, 21, 469-494, 2005.

[3] William K.J., Citto C., Shing P.B. Recent results on masonry infill walls. Advanced Mat. Research, 133-134, 27-30, 2010.

[4] Sarhosis V., Tsavdaridis K., Giannopoulos G. Discrete Element Modelling of masonry in-filled steel frames with multiple window openings subjected to lateral load variations. Open Constr. Build. Technology J., 8(1), 93-103, 2014.

[5] Choudhury T., Kaushik H.B. Seismic response sensitivity to uncertain variables in r.c. frames with infill walls. J. Struct. Eng., 144(10), 04018184 1-16, 2018.

[6] Fardis M., Bousias S., Franchioni G., Panagiotakos T. Seismic response and design of RC structures with plan-eccentric masonry infills. Earthquake Eng. Struct. Dyn., 28(2), 173-191, 1999.

[7] Perrone D., Leone M., Aiello M.A. Non-linear behaviour of masonry infilled rc frames: influence of masonry mechanical properties. Eng. Struct., 150, 875-891, 2017.

[8] Merino R. J., Perrone D., Filiatrault A. Consistent floor response spectra for performance-based seismic design of non-structural elements. Earthquake Eng. Struct. Dyn., 49, 261-284,2020.

[9] D.M.17.01.2018, Aggiornamento delle «Norme Tecniche per le Costruzioni», Ministero delle Infrastrutture e dei Trasporti, G.U. n.42, 20.02.2018 (in Italian).

[10] Gara F., Carbonari S., Roia D., Balducci A., Dezi L. Forthcoming. Seismic retrofit assessment of a school building through operational modal analysis and f.e. modelling. Journal of Structural Engineering (ASCE). doi:10.1061/(ASCE)ST.1943-541X.0002865

[11] Ormani R., Hudson R.E., Taciroglu E. Story-by-story estimation of the stiffness parameters of laterally-torsionally coupled buildings using forced or ambient vibration data: II. Application to experimental data. Earthquake Eng. Struct. Dyn., 41, 1635-1649, 2011.

[12] Astroza R., Ebrahimian H., Conte J.P., Restrepo J.I., Hutchinson T.C. Influence of the construction process and nonstructural components on the modal properties of a five-story building. Earthquake Eng. Struct. Dyn., 45(7), 1063-1084, 2016.

[13] Erazo K., Moaveni B., Nagarajaiah S. Bayesian seismic strong-motion response and damage estimation with application to a full-scale seven story shear wall structure. Eng. Struct., 186, 146-160, 2019.

[14] Stafford-Smith B., Carter C. A method for analysis for infilled frames. Proc. Inst. Civ. Eng., 7218, 31-48, 1969.

[15] Mainstone R.J. Supplementary note on the stiffness and strength of infilled frames. Current Paper CP 13/74, Building Research Station, Watford, U.K., 1974.

[16] Crisafulli F.J., Carr A.J. Proposed macro-model for the analysis of infilled frame structures. Bull. N. Z. Soc. Earthquake Eng., 40(2), 69-77, 2007.

[17] Vicente R., Rodrigues H., Arede A., Varum H. Simplified macro-model for infill masonry walls considering the out-of-plane behaviour. Earthquake Eng. Struct. Dyn., 45(4), 507-524, 2016.

[18] Di Trapani F., Shing P.B., Cavaleri L. Macroelement model for in-plane and out-of-plane responses of masonry infills in frame structures. J. Struct. Eng., 144(2), 1-13, 2018.

[19] Preti M., Bolis V., Stavridis A. Seismic infill-frame interaction of masonry walls partitioned with horizontal sliding joints: analysis and simplified modeling. J. Earthquake Eng., 23(10), 1651-1677, 2019.

[20] Mehrabi A.B., Shing P.B. Finite element modelling of masonry-infilled RC frames. J. Struct. Eng., 123(5), 604-613, 1997.

[21] Koutromanos I., Stavridis A., Shing P.B., Willam K. Numerical modelling of masonry-infilled RC frames subjected to seismic loads. Comp. Struct., 89(11-12), 1026-1037, 2011.

[22] Mazza F. In-plane-out-of-plane non-linear model of masonry infills in the seismic analysis of r.c. framed buildings. Earthquake Eng. Struct. Dyn., 48(4), 432-453, 2019.

[23] Braga F., Manfredi V., Masi A., Salvatori A., Vona M. Performance of non-structural elements in r.c. buildings during the L'Aquila, 2009 earthquake. Bull. Earthquake Eng., 9(1), 307-324, 2011.

[24] Vicente R., Rodrigues H., Varum H., Costa A., Silva J. Performance of masonry enclosure walls: lessons learned from recent earthquakes. Earthquake Eng. Eng. Vib., 11(1), 23-34, 2012.

[25] Penna A., Morandi P., Rota M., Manzini C., Porto F., Magenes G. Performance of masonry buildings during the Emilia 2012 earthquake. Bull. Earthquake Eng., 12(5), 2255-2273, 2014.

[26] De Luca F., Woods G.E.D., Galasso C., D'Ayala D. RC infilled building performance against the evidence of the 2016 EEFIT Central Italy post-earthquake reconnaissance mission: empirical fragilities and comparison with the FAST method. Bull. Earthquake Eng., 16(7), 2943-2969, 2018.

[27] Magenes G., Calvi G.M. In-plane seismic response of brick masonry walls. Earthquake Eng. Struct. Dyn., 26(11), 1091-1112, 1997.

[28] Bosiljkov V., Page A., Bokan-Bosiljkov V., Zarnic R. Performance based studies of in-plane loaded unreinforced masonry walls. Masonry Int., 16(2), 39-50, 2003.

[29] Tomaževič M., Lutman M., Bosilijkov V. Robustness of hollow clay masonry units and seismic behaviour of masonry walls. Constr. Build. Mat., 20(10), 1028-1039, 2006.

[30] Frumento S., Magenes G., Morandi P., Calvi G.M. Interpretation of experimental shear tests on clay brick masonry walls and evaluation of q-factors for seismic design. Research Report EUCENTRE 2009/02, Pavia, IUSS Press, 2009.

[31] Petry S., Beyer K. Cyclic test data of six unreinforced masonry walls with different boundary conditions. Earthq. Spectra, 31(4), 2459-2484, 2015.

[32] Salmanpour A.H., Mojsilovic N., Schwartz J. Displacement capacity of contemporary unreinforced masonry walls: an experimental study. Eng. Struct., 89, 1-16, 2015.

[33] Decanini L., Mollaioli F., Mura A., Saragoni R. Seismic performance of masonry infilled rc frames. Proc. 13th WCEE, Vancouver, Canada, 2004.

[34] Raka E., Spacone E., Sepe V., Camata G. Advanced frame element for seismic analysis of masonry structures: model formulation and validation. Earthquake Eng. Struct. Dyn., 44(14), 2489-2506, 2015.

[35] Wilding B.V., Beyer K. Force-displacement response of in-plane loaded unreinforced brick masonry walls: the Critical Diagonal Crack model. Bull. Earthquake Eng., 15(5), 2201-2244, 2017.

[36] Varum H., Furtado A., Rodrigues H., Oliveira J., Villa-Pouca N., Arede A. Seismic performance of the infill masonry walls and ambient vibration tests after the Ghorka 2015 Nepal earthquake. Bull. Earthquake Eng., 15(3), 1185-1212, 2017.

[37] Furtado A., Rodrigues H., Arede A., Varum H. Modal identification of infill masonry walls with different characteristics. Eng. Struct., 145, 118-134, 2017.

[38] Kouroussis G., Ben Fekih L., Conti C., Verlinden O. EasyMode: a MatLab/SciLab toolbox for teaching modal analysis. Proc. 19th Int. Cong. Sound and Vibration, Vilnius, Lithuania, 2012.

[39] Ewins D.J. Modal Testing: Theory, Practice and Application. Research studies press ltd, Baldock, Hertfordshire, England.

[40] EN1996-2. Eurocode 6: Design of masonry structures - Part 2: Design consideration, selection of materials and execution of masonry. European Community for Standardization, Brussels (2006).

[41] Mitchell A.K., Hazell C.R. A simple frequency formula for clamped rectangular plates. J. of Sound and Vibration, 118 (2), 271-281, 1986.

[42] Leissa A. W. The free vibration of rectangular plates. J. of Sound and Vibration, 31 (3), 257-293, 1973.

[43] Gorman D. J. Free vibration analysis of rectangular plates. Elsevier North Holland Inc., New York, 1982.

[44] Warburton G. B., Edney S. L. Vibrations of rectangular plates with elastically restrained edges. J. of Sound and Vibration, 95 (4), 537-552, 1984.

[45] Li W. L. Vibration analysis of rectangular plates with general elastic boundary supports. J. of Sound and Vibration, 273, 619-635, 2004.

[46] Allemang R.J., Brown D.L. A correlation coefficient for modal vector analysis. Proc. of 1st Int. Modal Analysis Conf., Bethel, CT, USA, 110–15 (1982).

[47] National Instruments. LabVIEW Signal Processing Course Manual. National Instruments Corporate Headquarters, 1997.

[48] Cantieni R. Experimental methods used in system identification of civil engineering structures. Proc. 1st Int. Operational Modal Analysis Conf., Copenhagen, Denmark, 249-260, 2005.

[49] Juang J.-N. Applied System Identification. Prentice-Hall Englewood Cliffs, New Jersey, USA, 1994.

[50] Van Overschee P., De Moor B. Subspace identification for linear systems: theory–implementation–applications. Dordrecht, The Netherlands: Kluwer Academic Publishers, 1996.

[51] Sandwell A., David T. Biharmonic Spline Interpolation of GEOS-3 and SEASAT Altimeter Data. Geophysical Research Letters, 2, 139-142, 1987.

[52] SAP2000 advanced (v20.2) Static and dynamic finite element analysis of structures, Berkeley, CSI Computer & Structures, Inc., 2018.